DEBRIS TORRENT MECHANISMS

by

K.J. SMYTH

B.Sc. Queen's University of Belfast, 1974

A THESIS SUBMITTED IN PARTIAL FULFILLMENT OF

THE REQUIREMENTS FOR THE DEGREE OF

MASTER OF APPLIED SCIENCE

in

THE FACULTY OF GRADUATE STUDIES

Department of Civil Engineering

We accept this thesis as conforming

to the required standard

THE UNIVERSITY OF BRITISH COLUMBIA

SEPTEMBER 1987

In presenting this thesis in partial fulfillment of the requirements for an advanced degree at the University of British Columbia, I agree that the Library shall make it freely available for reference and study. I further agree that permission for extensive copying of this thesis for scholarly purposes may be granted by the Head of my Department or by his or her representatives. It is understood that copying or publication of this thesis for financial gain shall not be allowed without my written permission.

Department of Civil Engineering

The University of British Columbia
2075 Wesbrook Mall
Vancouver, B.C.
V6T 1W5

Date: September, 1987

ABSTRACT

The phenomenon of the debris torrent is explored by examining the mechanisms of initiation, particularly those of rainfall and deforestation. The types of precipitation likely to contribute to instability are identified and data collection is reviewed.

Debris torrents have characteristics unlike that of ordinary stream flow, and are capable of transporting massive quantities and sizes of material. Models to explain this transport capability are compared and contrasted. A theoretical analysis of the flow regime is carried out which is argued to be consistent with the observed turbulent nature of a debris torrent. This analysis is extended to the calculation of super-elevation in bends and shows that current attempts to estimate velocities from super-elevation data may be very conservative.

Further application of the turbulent stress analysis is used to estimate the angle of spread of the debris torrent in the deposition zone, and this analysis may be useful in zoning the downstream area to safeguard construction.

TABLE OF CONTENTS

LIST OF TABLES

LIST OF FIGURES

LIST OF SYMBOLS

A	constant
a	constant
B	surface width of flow
C	cohesion/unit area
c'	cohesion intercept
c_*	grain concentration by volume in static debris bed
D	grain diameter
g	acceleration due to gravity
h	depth of flow
h_w	porewater pressure
k	constant
K	constant
m	fraction of depth such that M is the vertical height of ground water table above slip surface (Fig. 2.4)
p	pressure due to weight of solids and water
P	dispersive pressure
$\underline{\Delta P}_1, \underline{\Delta P}_2$	inflow, outflow pressure difference in mb
R_h	hydraulic radius
R	radius of bend
R_M	radius of centreline of stream bend
s	standard deviation of normal distribution
S_0	slope
T	shear stress
t	time
u	velocity of flow
$\bar{u}$	time averaged part of velocity u
u'	momentary fluctuation of velocity u
u_{*c}	critical shear velocity
V	velocity for calculation of thrust force
z	vertical depth of slip surface

LIST OF SYMBOLS (Continued)

α	dynamic angle of internal friction
β	angle of flow to face of barrier
γ_s	unit weight of solids
γ_w	unit weight of water
θ	slope angle
μ	viscosity
ρ	density of water
δ	density of grains
σ_n	normal stress
τ	shearing resistance/unit area
τ_y	yield strength
ϕ'	angle of shearing resistance
λ	linear concentration of particles

ACKNOWLEDGEMENT

I would like to take this opportunity to express my appreciation and thanks to my advisor Professor M.C. Quick for his advice and guidance during the research and the preparation of this thesis.

CHAPTER 1

INTRODUCTION

A debris torrent channel is often a relatively quiet mountain stream which under suitable conditions can become the transporter of massive material that has great destructive power.

The physical processes which give rise to a debris torrent are reviewed. Logically, they are sub-divided into geologic, meteorologic, and particle and hydrodynamic processes. Some of the geologic parameters are shown to be reasonably well defined. However, the rainfall necessary for the formation of a torrent is shown to be subject to considerable uncertainty, especially because of the lack of good data. The main emphasis of this thesis is on the particle and hydrodynamics of the debris movement. The physical interactions of the solid and fluid components are re-analyzed and it is argued that peak velocities of debris movement may have been underestimated. A consequence of this underestimation would be a major revision of estimates of impact forces and possible damage to structures.

The effects of debris torrents are manyfold, ranging from the disasters to property and life, by the movement of large boulders, to the long term buildup of landforms by the formation of debris fans in the river valleys.

Debris torrents contribute to the formation of alluvial fans. The widespread, perhaps dominant, influence of this mechanism in the natural evolution of landforms has gone largely unrecognized owing to the long recurrent interval between events (Campbell, 1975).

A debris torrent can quickly fill basins behind small check dams rendering them ineffective in controlling subsequent surface runoff.

The effects on small residential dwellings range from quiet inundation to complete destruction. Flows of sufficient volume and momentum have smashed structures into pieces and move foundations, for example in Alberta Creek, British Columbia: "Damages included total destruction of three houses and structural damage to one other house and carport... Five culverted road crossings were washed out and Highway 99 bridge was swept off its foundations." (Woods, 1983). In other instances, buildings have had layers of muddy debris deposited inside them, commonly accompanied by little structural damage. Apparently the debris was moving at relatively low velocities; the flows entered the dwellings through open doors or windows and quietly flooded the interiors.

It is also worth noting that the size of the boulders (and hence the destructive ability) depends on the character of the bedrock, i.e. volcanic rock will contribute large boulders, whereas a weak sandstone will only contribute clasts of pebble size.

A debris torrent may cause the channel to shift, especially in the downstream depositional region. This channel shifting can be triggered by the

1) sediment load, which varies greatly with debris torrent surges.
2) local deposition during lulls in the storm, or between torrents, may fill the old channel and divert subsequent flow into a new one, or cause flooding of the fan remote from the pre-existing stream channel,
3) During deposition debris levees tend to form along the channel boundaries and these levees may channel or divert subsequent flows.

Channel bends are a particular hazard region, for example, in the Alberta Creek torrent of February 1983 the confines of the channel were unable to contain the torrent on the bend causing part of the debris to leave the channel and bury a recreational vehicle with subsequent loss of life.

The literature is filled with tragic case histories like that of Alberta Creek, but unfortunately these dangers are not always obvious, since the periodicity of debris torrents is irregular on any individual creek and long periods of dormancy often permit full re-establishment of forest cover over affected areas.

In the following chapters, the processes which give rise to a debris torrent will be reviewed. In particular, the precipitation necessary to initiate a torrent will be considered and the rainfall data network density needed to define the rainfall will be considered. Consideration will then be given to the dynamics of the sediment motion and Bagnold's dilatant fluid model will be compared with the plastico-viscous rheological model. The Bagnold model is then used to analyze velocity distribution and special application is made to the flow in a bend. This analysis indicates that peak velocities of debris may be higher than previously estimated and therefore impact loads may be considerably higher.

CHAPTER 2

INITIATION IN SOURCE AREA

2.1 Instability Due to Rainfall

In order for a debris torrent to be initiated there must be sufficient material in the form of mud, rocks, sand and branches combined with an amount of water available to the creek bed. This material is transported to the creek by land movements from what we will call debris source area of the creek (Fig. 2.1).

The transport of material into a creek bed is tied to the correlation between debris torrent activity and moderate to heavy rainfall. Once sufficient water makes it unstable the source material moves in debris slides, avalanches or debris flows, making its way into the creek.

This sliding of material results from the interaction of infiltration and downward percolation at depth, (Kesseli, 1943), where the former takes place at a rate greater than the latter, the water content of the top zone will increase to a critical point at which sliding will originate. When infiltration through the regolith[1] exceeds the transmissive capacity of the rocks below, a temporary perched water table is formed (Campbell, 1975). The head will continue to increase, with continued rainfall, until all the surficial zone is saturated, after which all the rainfall in excess of the transmissive capacity of the bedrock is distributed as surface runoff and downslope seepage. The

[1]The loose incoherent mantle of rock fragments and soil which rests upon the bedrock.

association of debris slides with rainstorms is clear evidence that slope-mantle materials that are stable under "normal" conditions become unstable during rainfall of sufficient duration and intensity.

For any site it is possible to establish limiting slopes at which soil slips are unlikely and an upper slope above which retention of a continuous mantle of colluvium would not be possible (Fig. 2.2) (Campbell, 1975). This data is, of course, specific to the Santa Monica Mountains where the range of 12° to 56° are limiting angles. These limiting angles depend on local geology and should be established on a site specific basis. Figure 2.3 shows an idealized debris source area as the conditions for land movement are being reached, in which shallow rooted vegetation with a thin mulch of dead leaves and grass growing in a regolith of colluvial soil, the upper part of which contains abundant living and dead roots as well as animal burrows. When the rate of infiltration into and through the upper layers is equal to or less than the capacity of the bedrock to remove it by deep percolation, the water moves towards the permanent water table below and the stability of the slope material is not affected. On the other hand if this deep percolation is less than the infiltration a perched water table is formed and will continue to rise until surface runoff and downslope seepage takes place.

The criterion for failure of a soil slab is that the ratio of the tangential and normal forces must exceed a critical value, which is dependent on the type of material.

The effect of the addition of water in changing a slab of the source material from stable to unstable may be explained using the formula (Terzaghi, 1950, p.92),

$$\tau = c + (p - hw)\tan\phi$$

where

τ = shearing resistance/unit area

ϕ = angle of internal friction

hw = porewater pressure

p = pressure due to weight of solids and water

c = cohesion/unit area

The decrease in shearing resistance, when a water saturated zone forms above the slip surface is evident if we consider the component of cohesion c (which is really apparent cohesion obtained from the air-water surface tension), this is reduced to zero as the water takes the place of air in the interstices and also the term (p-hw) is decreased due to increase in piezometric head.

A formula developed by (Skempton and DeLory, 1957) for the condition that ground water flow is parallel to the slope at shallow depth gives the Terzaghi equation in more readily measured soil parameters,

$$F = c' + \frac{(\gamma_s - m \cdot \gamma_w) z \cos^2\theta \tan\phi'}{\gamma_s z \sin\theta \cos\theta}$$

where

F = factor of safety

c' = cohesion intercept

z = vertical depth of slip surface

m = fraction of z such that mz is the vertical height of ground water table above slip surface (Fig. 2.4)

θ = slope angle

γ_s = unit weight soil

γ_w = unit weight water

ϕ' = angle of shearing resistance

For the special case of c' = 0 the critical slope is given by

$$\tan\theta_c = \frac{\gamma_s - m\,\gamma_w}{\gamma_s} \tan\phi'$$

i.e., F=1.

It is now possible to show a family of curves for F=1, for various combinations of soil parameters γ and $\tan\phi'$ (Fig. 2.5) from which the critical angle θ can be determined.

This is however an idealized situation although such curves prepared for a given site should permit a preliminary evaluation of recurrence interval for failures due to rainstorms. The recurrence interval for values of m at F=1 can be approximated from recurrence intervals for rainstorms of sufficient intensity and duration provided thickness and infiltration rates of regolith are known. If infiltration rates are low, duration of rainfall will be dominant and if they are high, intensity should be dominant.

A study (Sidle and Swanston, 1982) on debris slides in coastal Alaska used much the same approach. They noted the great oversimplification in using a linear slope model which ignores many complex field situations. They found unreasonably high values of ϕ', suggesting that cohesive properties existed in the soil mantle. A multistage triaxial test was performed on an undisturbed sample on a site adjacent to the failure, giving a much lower and more reasonable value of ϕ'. When this

value was substituted in the equation a positive value of c' was obtained. This was attributed, at least in part, to root strength of the vegetation.

It is important to note that for relatively thin soils in steep terrain where the effective normal forces are low, small changes in apparent cohesion will have a dramatic influence on the factor of safety (Sidle and Swanston, 1982). For this site, based on a porewater pressure at failure of 2.17 kPa the factor of safety calculated for c' = 1.0 and 5.0 kPa were 0.75 and 1.73, respectively.

This relationship between c' and factor of safety for thin soils indicates that even small values for rooting strength and true soil cohesion can be critical in determining the stability of these steep slopes.

2.2 Instability Due to Removal of Forest Cover

An important factor in the creation of instability in the debris source area is the removal of forest cover by logging or fire.

The effects of logging have been studied by many researchers and is surrounded by much controversy. These effects are:

Eisbacher, 1982

- Intact forest absorbs some of the rain during storms and results in less or at least delayed runoff.
- A living system of roots binds the colluvium to the substratum, adding some strength to the slope.

Aulitzky, 1974 notes that:

- Rooting strength is decreased which possibly released creep generated stresses in the soil root complex.

- Transpiration is decreased.
- Shading of snowpack is lost, increasing runoff.
- Interruption of surface drainage associated with road surfaces, ditches and culverts.
- Alteration of subsurface water movements especially where road cuts intersect the water table.
- Change in distribution of mass on a slope surface by cut and fill construction.

It seems that the problem of large clearcutting is generally compounded by unmanaged access roads which commonly are the first sources of debris into the adjacent creek.

It was found (Aulitzky, 1974) that in Alpine areas, slides in unstable regions transported a two to eight times greater volume of material when clearcut than did those where forest cover was maintained. He also found that the combined impact of roads and clearcut logging constituted a five-fold increase in erosion relative to undisturbed forested areas.

In a study for protection works against debris movement at Port Alice, B.C. (Nasmith and Mercer, 1979) it was noted that much of the slope above the town was logged prior to construction of the town and that the debris movement had started at an upper logging road.

It was concluded (Eisbacher and Clague, 1981) that deforestation due to urbanization and clearcut logging may increase the incidence of debris avalanches and slides on moderate to steep slopes. In addition, logging debris along stream courses may impede surface drainage and cause additional slope failures.

Another cause of forest cover removal is fire. Often in the dry season vegetation cover is highly flammable and if the watershed is burned and precipiation between the fire and the first storm is low, little vegetative recovery is possible (Scott, 1969). Consequently when a storm hits the initial rainfall would be absorbed by the dry soil mantle and the watershed rapidly saturated. When the next storm hits conditions are ideal for slope failure.

In a study of flood erosion in L.A. county it was found (Eaton, 1936), that when the watershed cover was destroyed erosion rates increased by fifty to one hundred times over that with undisturbed vegetative cover and that the best protection from debris is the normal vegetative cover. After denudation, any protection program is secondary, far less efficient and much more costly.

2.3 Instability from Other Causes

Terzaghi (1950) examines land movement in detail and cites the following causes of instability:

- Undercutting of the foot of the slope or deposition of earth or other material along the upper edge of the slope. Both operations produce an increase of shearing stresses on the ground beneath the slope. When the average shearing stress on the potential slide surface becomes equal to the average shearing resistance a debris slide occurs.
- Earthquake shocks increase the shearing stress along the potential surface of the sliding whereas the shearing resistance remains unchanged.

All the researches cited agree that precipiation is the essential ingredient in causing instability in the debris source area and that disturbance of the watershed by deforestation and its attendant construction can not only accelerate the phenomenon but increase the amount of debris available to the torrent channel.

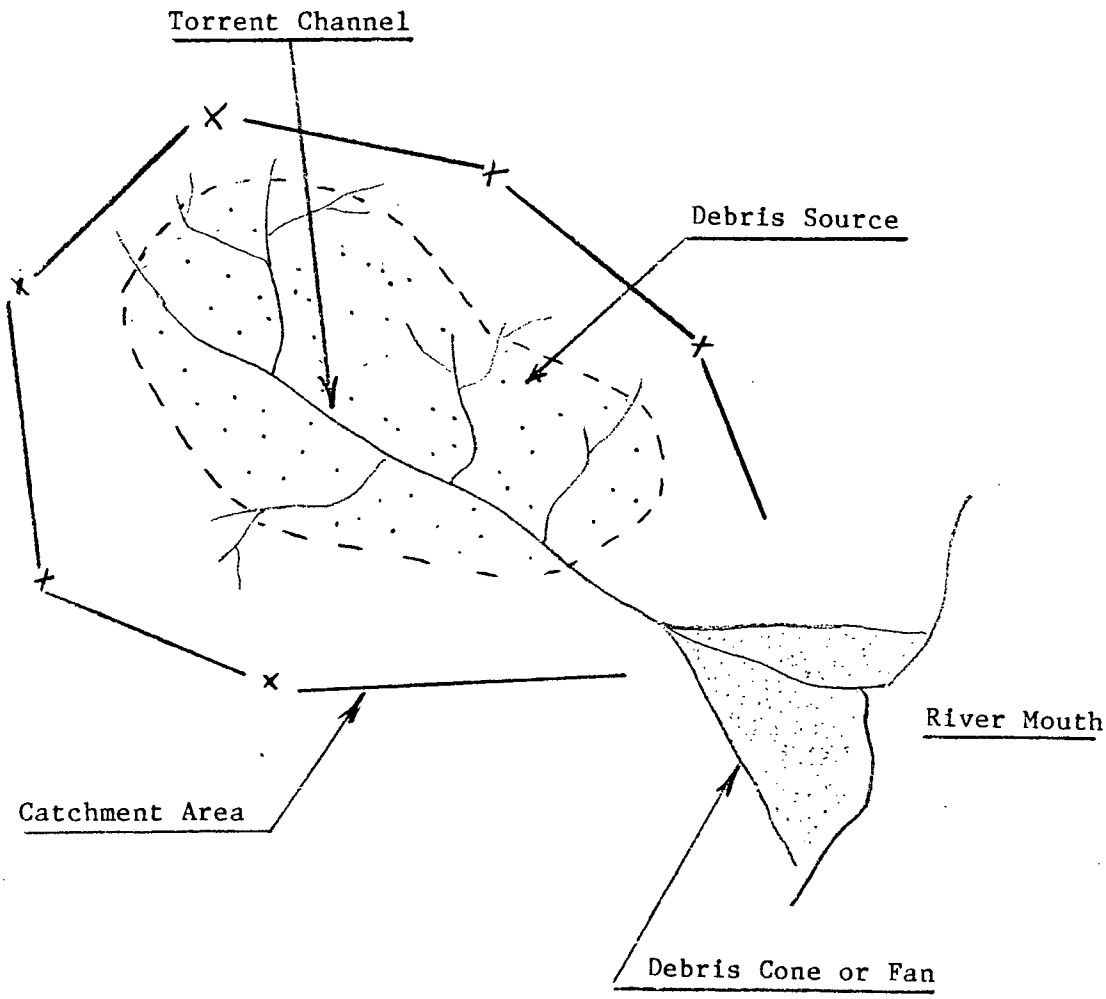

Figure 2.1 Characteristic of debris source area
(Campbell, 1975)

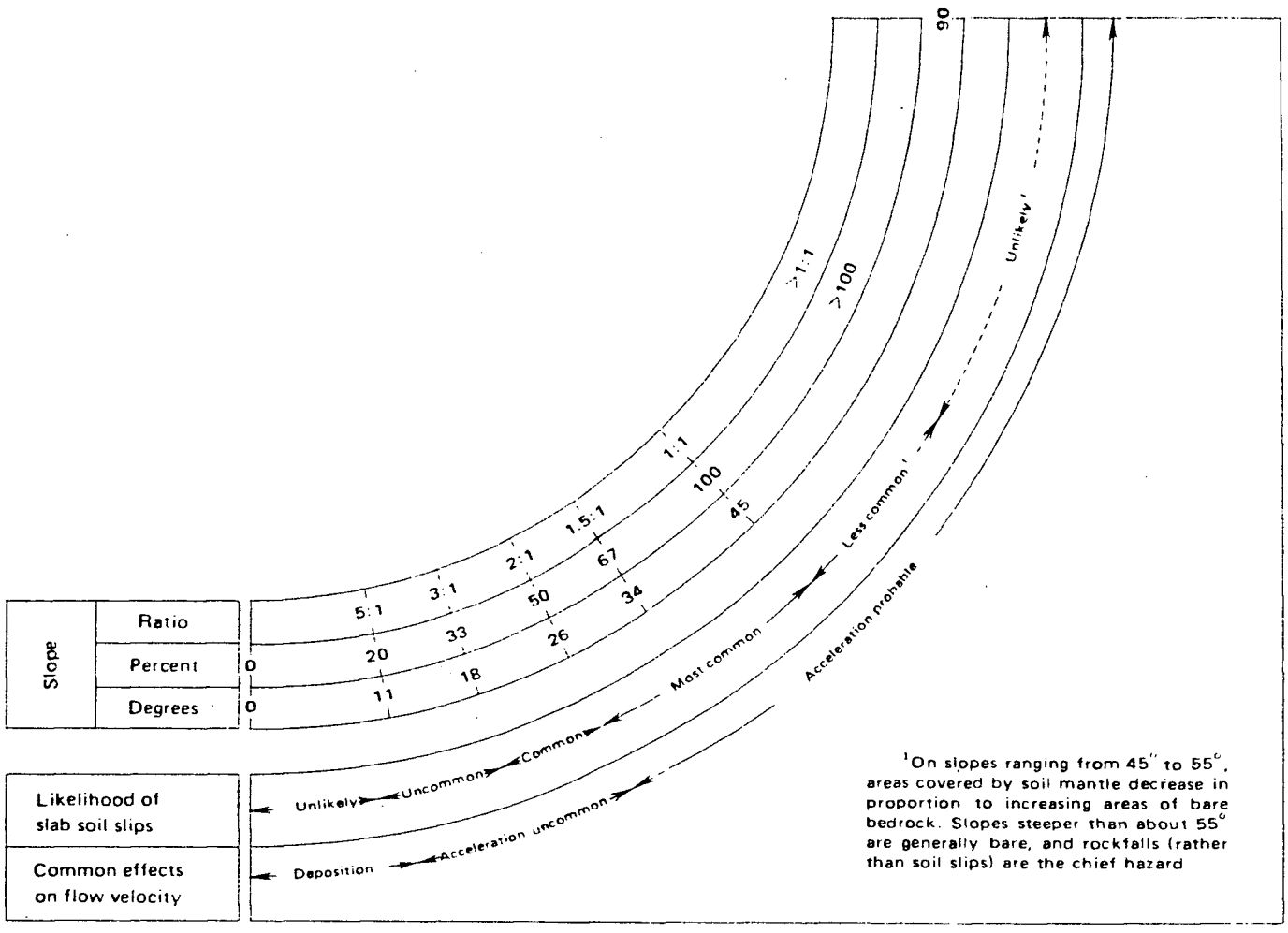

Figure 2.2 Limiting slopes for soil slips, Santa Monica mountains (Campbell, 1975).

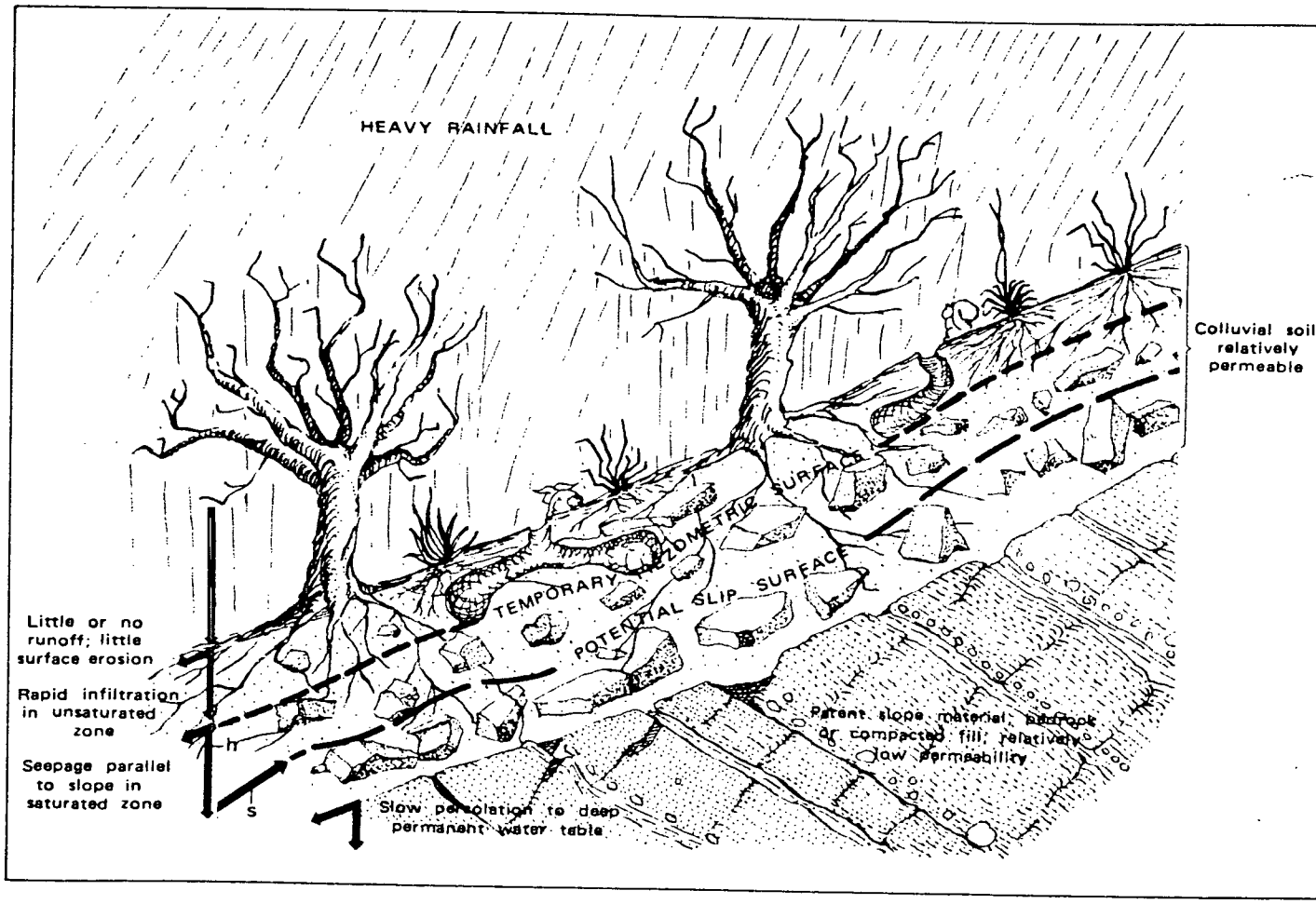

Figure 2.3. Diagram showing buildup of perched water table in colluvial soil during heavy rainfall (Campbell, 1975).

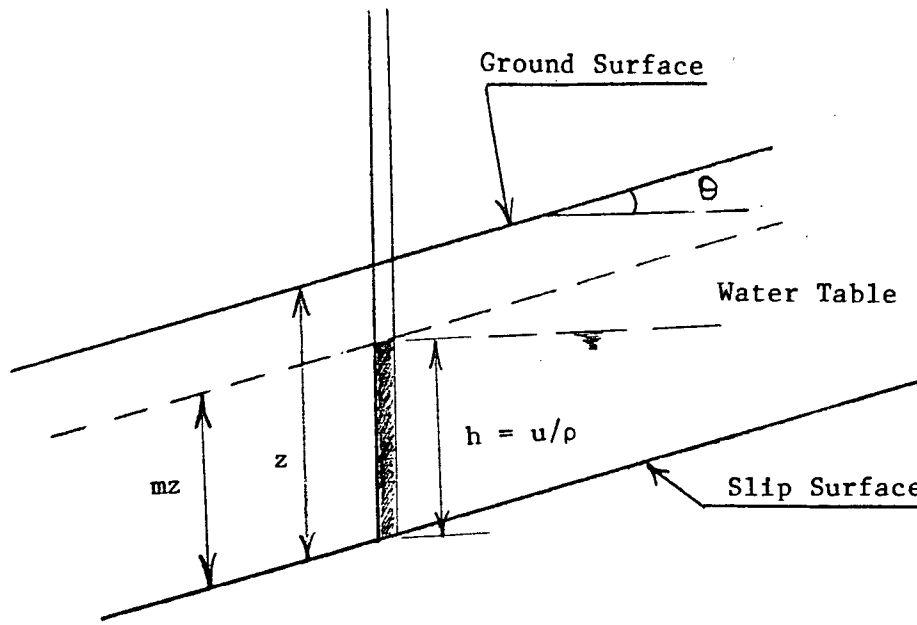

Figure 2.4. Diagram showing z such that mz is the vertical height of ground water table above slip surface (Campbell, 1975).

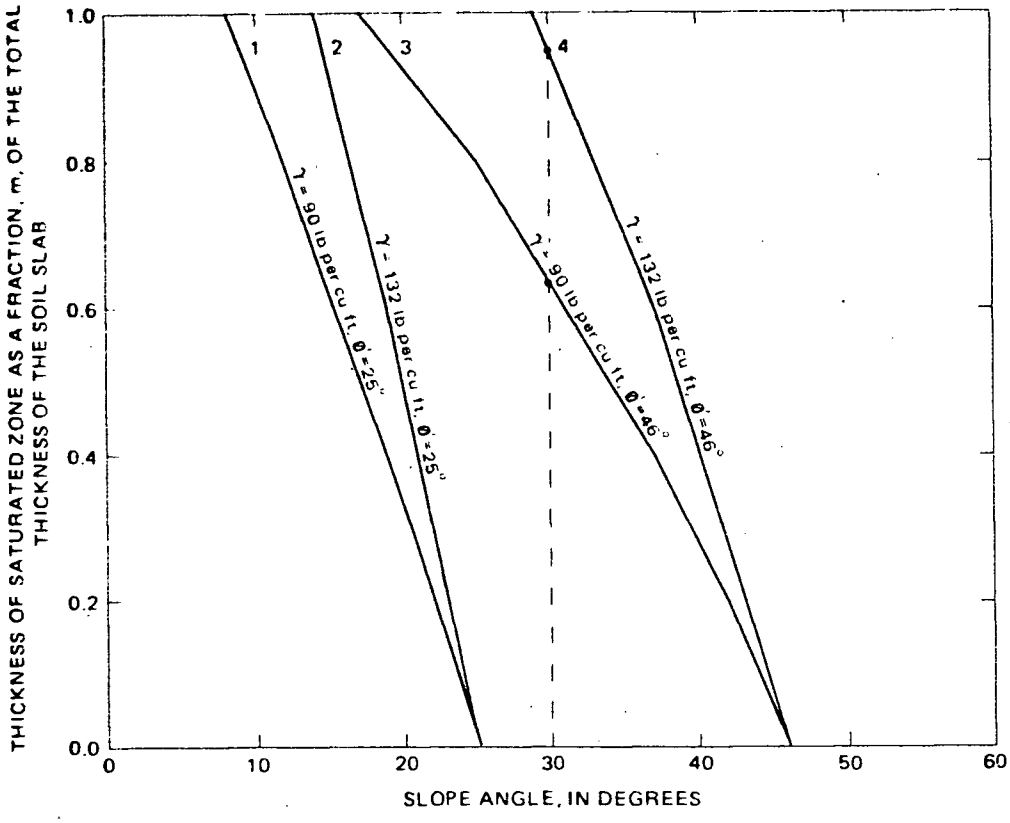

Figure 2.5. Relation of failure in some typical soils to ground water content and slope angle. Computed curves for F=1 (failure criterion) at selected values of γ_s and ϕ'. The curves for most natural nonclayey soils lie between curves 1 and 4. Fields to the left and right of each curve are stable and unstable, respectively (Campbell, 1975).

CHAPTER 3

PRECIPITATION

3.1 Classification

Meterologists have adopted a qualitative classification scheme and view precipitation phenomena on 3 scales.

3.1.1 Synoptic or Macroscale

Storms which are discernable on weather satellite photographs, associated with low pressure and frontal systems. They are generally in the order of hundreds of kilometers in size. In the Vancouver area they are usually in the form of cyclonic systems moving eastward of the Pacific Ocean.

3.1.2 Mesoscale

Within the band of precipitation from the synoptic system is a "pebbly structure" as seen by radar (Bonser, 1982), of patterns of precipitation. Generally they are typically 10 to 50 km in extent, up to 60 km apart and move in step as the band of precipitation sweeps over the earth. Thunderstorms are an example of a mesoscale system.

3.1.3 Microscale

Convective cells which are responsible for intense bursts of rainfall over short time intervals. They range from 2 to 10 km across and last up to an hour. They are generated by a local instability in the atmosphere, grow rapidly and often contain strong updrafts and downdrafts.

Types of precipitation are classified in 3 principal categories (Bonser, 1982):

Cyclonic - Rainfall arises when moist air masses in a frontal system rise due to the horizontal convergence of envelopes of air having different temperatures.

Orographic - Rainfall is caused by lifting of the air mass by topographic features such as mountain barriers. The maximum amount of precipitation comes on the middle part of the slope of a high mountain (Yoshino, 1975).

Convective - Differential heating of adjacent air masses generate local instability. Individual convective cells form within the broad rainfall areas and appear to remain in position relative to the broad rainfall areas. Cells remain identifiable for between 30 and 60 minutes. Peak intensities are usually observed to be of 10 minutes or shorter.

Progression of these systems across the B.C. coast have been followed by radar and it was concluded by Bonser (1982): "It is only by observing these patterns that one begins to appreciate the complexity inherent in the precipitation, a complexity not at all apparent from conventional hyetograph records."

3.2 Data Collection

When one considers the areas subject to debris torrent activity, i.e., the steep upper reaches of small drainage basins, these variations in precipitation patterns become very important. The literature indicates basins subject to torrent activity ranging in area from 0.03 to

0.17 km² (Scott, 1969), while in Howe Sound they range from 0.4 to 4.7 km². These small basins have the size and location to be influenced significantly by the cellular and orographic effects noted above.

Current practice is to analyse point rainfall data by ignoring the movement of storms, assuming a stationary growth and decay, or to consider a constant rainfall rate over an area for a critical time period. An explicit consideration of storm growth, velocity and track is a preferable approach but this requires knowledge of the spatial and temporal variation of precipitation.

In the Howe Sound area the data coverage is biased towards low elevation sites, most stations are located along the major transportation routes and the large block of mountains between the Fraser Canyon and Highway 99 has data coverage only along its southern margin.

The measured amount of rainfall in a mountainous area differs considerably according to the method of observation and equally great differences arise according to the density and position of observation points because of the great local variability of rainfall. A study from Japan (Yoshino, 1975) shows the results of studies in the vicinity of Isohara. Table 3.1 shows the statistics of every rainfall of over 30 mm per one cyclone from September 1950 to September 1951. This table shows the large errors inherent in a sparse gauging network.

Miles and Kellerhals (1981) investigated a debris torrent in the region of Hope, B.C. for the period of December 26-27, 1980, and estimated that the rainfall of 75 mm in 25 hours, measured at valley bottom, to have a return period of 2 to 5 years whereas the flood discharges from the same storm indicated a 50 year return period. It was concluded that this rather large water deficit was made up from the "condensation

of melting snow". In the same paper they conclude that based on valley bottom precipitation the return period for a debris torrent design rainfall of 150 mm in 24 hours would be upwards of 50 years but they note that short term data collected in the mountain passes by the B.C. Ministry of Highways indicate that this rainfall has a recurrence period of 15 years. It would seem possible that the main causes of these high runoff events is due to cellular and orographic phenomena which are not reflected in the lower level gauges, as Bonser (1982) concludes, "it is the microscale precipitation which is most responsible for these peak runoff responses in small watersheds".

Apart from the areal distribution of the gauges it is important to consider the temporal nature of these high intensity events. Since these high intensity cells can last for less than one hour, the hourly rain gauge can miss the peaks within the hour period. A comparison of hourly data and 10 minute radar data (Bonser, 1982) used in an urban runoff model showed that the peak runoff from the hourly data underestimated that from the 10 minute radar measurements by a factor of 3, and although the timings of peaks agree, all those for the hourly data show lower flows. This is due to the averaging of peak intensities in the hourly records (see Fig. 3.1).

The Vancouver area exhibits strong orographic controls (Shaeffer, 1973). In a storm analysis of July 1972 it was shown that while 50 mm fell at Delta Tsawwassen Beach over 250 mm fell at Hollyburn Ridge, el. 930 m. In the lower Fraser Valley much annual precipitation is produced by vigorous frontal storms similar to the one in question and Shaeffer (1973) contends that the rainfall distribution of such a storm should resemble the distribution of mean annual precipitation since orographic

controls are fixed. A comparison of published maps of mean annual precipitation over the lower Fraser valley (Wright, 1966) supported this contention. Thus over most of the area inferences concerning orographic influences could bear relationships to these represented by mean annual distribution. Rainfall rates for the same storm were calculated by dividing total precipitation at each point by the duration, which also increased with elevation and it was found that intensities doubled between sea level and the mountains north of the city. These are general trends and should be considered where return periods are being estimated from valley bottom data, but due to the sparcity of the data points, they should not be expected to apply to every storm since parameters such as wind speed, wind duration, cloud type and cloud height can affect the orographic component.

The B.C. Water Resources and C.A.E.S. operated 10 instrument sites across the Beaufort Range on Vancouver Island. The available results showed a general increase in precipitation with elevation, horizontal variations being significant at all levels and indicating that local variations in exposure, slope and aspect are important (Table 3.2).

The Department of Highways have installed rain gauges at upper elevations in the Howe Sound area, but they have been malfunctioning and, the data collect so far is not useful. When these gauges are operating they may give the information required to estimate the rainfall events that trigger torrent events. As it is we can say, that in these high elevation catchments prone to torrents, the orographic influences are significant and produce greater amounts of precipitation than our available gauging networks show. This coupled with high intensity cellular activity are the major contributing factors in debris torrent

initiation. Sustained greater durations and intensities leave field conditions (ground water levels) requiring perhaps only a short intense burst of rainfall to cause instability. Such intense cellular activity may not pass over the gauges.

Thurber (1983) questions this on the basis that their information indicates that these cells appear to have dimensions in the order of 10 km or greater. However, there may be greater variation in size, (Bonser, 1982; Penny, C.A.E.S. pers. comm.). They suggest that these cells may indeed be as small as 1.5 km. Thurber concludes, "If there had been exceptionally high rainfall intensities associated with most of the events in the study area, similarly high intensities would have been recorded nearby at least on some occasions" and that, "there is no conclusive evidence that climatic conditions alone have controlled the occurrence of debris torrents".

However, in Japan, studies have shown that debris slides and landslips are strongly correlated with heavy rain. In one study (Yoshino, 1975) it was found that the areal distribution of density of landslides in the central part of the landslides does not correspond to the distribution pattern of the degradation density classification by rocks, but it closely correlated to the rainfall distribution and that when the amount of rainfall surpassed a certain limit any slope with a gradient of 30°-50° is subject to landslide regardless of the difference in geological features. In another study, (Yoshino, 1975) it was confirmed that the areas with most frequent landslides nearly coincide with the areas where the maximum rainfall exceeds 10-15 mm/10 minutes or 30-50 mm/hour.

Although there may be other contributing factors that may aid the process and increase the extent of land movement there is a vast amount of evidence to support the belief that rainfall is the decisive factor in the occurrence of debris slides and debris torrents (Eisbacher, 1982; Eaton, 1936; and Campbell, 1975). In addition it appears that many of these rainfall events are outside the scope of our present measurement facilities. Attempts to take the available valley bottom data and from it predict rainfall rates and durations at higher elevations is a complicated procedure requiring some caution.

3.3 Precipitation Network

As suggested earlier the gauging networks in British Columbia are quite sparse and in higher elevation zones, generally non-existent. To put this into a world context, Ferguson (1973) has provided guidelines for the density of precipitation, snow course, hydrometric and evaporation networks for various classes of physiographic and climatic conditions (see Table 3.3). This table indicates that except for arid or polar regions, average precipitation network densities in mountainous regions should be approximately 3 to 6 times as large as those in flat terrain. Table 3.4 provides information on current precipitation networks in a number of countries and only Switzerland meets or exceeds the WMO specification. The important area to note is that of B.C. and by reference to Figs. 3.2 and 3.3, we see that the precipitation network in B.C. falls very far below the WMO recommendations, with most stations in low lying areas, below 600 m.

A major problem in all areas is the relative sparseness of data at high elevation. Stations tend to be concentrated at valley locations as seen in Fig. 3.3.

3.4 Predicting Orographic Effects

There are a number of models that can predict to some degree what the orographic effects of a mountain barrier may be. A simple linear model is used by the World Meterological Organization (W.M.O., 1973). If it is assumed that the air is saturated and that temperature decreases along rising streamlines at the moist adiabatic rate, and the flow is treated as a single layer of air between the ground and the nodal surface, between 400 and 100 mb where the air flow is assumed horizontal, the rate of precipitation is

$$R = \bar{V}_1 \frac{(W_1 - W_2 \frac{\Delta P_1}{\Delta P_2})}{Y}$$

where

R = rainfall rate in cm/sec

$\bar{V}_1$ = mean inflow wind speed in cm/sec

W_1, W_2 = inflow and outflow precipitation water in cm (liquid water equivalent) found from tables of precipitable water in a saturated pseudo-adiabatic atmosphere (W.M.O., 1973)

Y = horizontal distance in cm

$\Delta P_1, \Delta P_2$ = inflow and outflow pressure differences in mb

The model considers the flow of air in a vertical plane at right angles to a mountain chain or ridge (Fig. 3.4). From the equation one can see the variation of orographic effects with wind direction and temperature.

This model is highly simplified as it is well known that all the condensate does not fall out on the mountain barrier. Thus the "efficiency" with which the condensate is removed is less than one. The measure for the condensate is the precipitable water which expresses the total mass of water vapour in a vertical column of the atmosphere, to say that the air contains 3 cm of precipitable water signifies that each vertical column of 1 cm^2 cross-section contains 3 gm of water in vapour form. If the water vapour were all condensed into liquid water and deposited at the base of the column the accumulated liquid would be 3 cm deep. No natural process will precipitate all the water vapour in the atmosphere.

There appears to be an elevation range where this "efficiency" is maximum and related to a specific cloud type (Elliot, 1977). When data from the Blue Canyon, California was plotted against that calculated by the W.M.O. model a marked increase in efficiency was found at approximately 1250 m (Fig. 3.5).

Whitmore (1972), in examining the effects of altitude on precipitation in South Africa concluded that mean annual rainfall increases fairly steadily up to about 1300 m, above which altitude the rainfall increases only slightly. Lessman et al. (1972) found that, as water vapour decreases with height, tropical rainfall increases with height only up to a certain level and decreases with additional height, these features vary with extent, slope and orientation of the barrier, its location relative to humidity sources, prevailing wind directions and velocity as well as the vertical extent and degree of stability of the humid layers in the atmosphere and (Shaw, 1972) found that all the meteorological characteristics are greatly influenced by altitude, and

aspect has an added effect on precipitation. Temperature and humidity decrease with height and above the layer of maximum cloud development (1000-2000 m) humidity drops off significantly. On reaching plateaus in high mountains rainfall and cloud amounts become less and the intensity of rain diminishes. A more sophisticated model which attempts to take this "efficiency" into account was developed by U.S. Dept. of Commerce, Office of Hydrology (Elliot, 1977). He states that the "efficiency" varies with the characteristics of the orographic cloud, especially with respect to its cloud top temperature since this is a measure of the abundance of the available ice-forming nuclei that get the precipitation process started. The "efficiencies" associated with various cloud formations must be found by reference to actual storm data that include, besides precipitation rates, frequent sounding data from the immediate upwind valley. The model depends in a complex way upon character of the terrain, the efficiency with which the microphysical mechanisms remove cloud condensate as precipitation, the wind direction and speed the depth of cloud and the air mass stability. It gives a transferable method of computing mean areal precipitation over basins where the real time precipitations data is limited such as B.C.

The output of the program is a grid point map of the efficiency, which represents a prediction of the orographic component of precipitation over the barrier times a number that is constant over the entire grid for a given case. In order to use this map it is necessary to adjust the magnitude at grid points by the use of an observed precipitation value. The input e (efficiency) measures the fraction of cloud water that is removed as precipitation and is assumed constant over the entire barrier for any given cloud type. The model identifies four

basic cloud types, stable warm, stable cold, unstable warm, and unstable cold (unstable if the positive area on the thermodynamic chart extends through a layer deeper than 75 mb and warm if cloud top temperature over the barrier is warmer than -30°C).

The results show a fair correlation in some sites but poor in others where"barrier wind effects are too complex for the model". One should note however that while other researchers note a marked change in efficiency with altitude this model assumes it constant for a given cloud type.

This model uses 37 parameters in all and if the data required were available and it could be "tuned" to the Howe Sound area it would be a great aid in dealing with the unmeasureable orographic component of precipitation that is so important in the debris torrent situation.

The Howe Sound situation requires estimation of these orographic effects, but the models examined all have shortcomings, certainly a linear extrapolation of valley bottom data may be useful for annual precipitation, but for an individual storm this does not take into account the many other parameters. At present the data collection network does not enable us to correlate the actual basin precipitation with torrent events and until such time as the network is expanded a return period prediction based on synoptic patterns is impossible.

Number of Stations	3	6	9	12	15	18	21	24
Area Per Station km^2	280	140	90	70	60	50	40	35
Error %	25	18	13	10	8	6	5	3

Table 3.1 Errors inherent in sparse gauging network (after Yoshino, 1975)

STA	El(m)	Relative Precip. to A %
A	425	100
B	842	106
C	1395	147
D	740	110
E	425	75
F	425	88
G	750	102
H	1380	165
I	760	116
J	425	73

Table 3.2 Data from Beaufort Range, Vancouver Island.

Table 3.3

Network specifications recommended by WMO (1970).
Figures show maximum specific areas (inverse of network density) in km² per station.
Provisional networks may be tolerated under difficult conditions.

TYPE OF REGION	PRECIPITATION		SNOW COURSES	HYDROMETRIC		EVAPORATION
	Range of Norms	Provisional		Range of Norms	Provisional	
1. Flat regions of temperate mediterranean and tropical zones.	600-900	900-3000		1000-2500	3000-10,000	
2. Mountainous regions of temperate mediterranean and tropical zones.	100-250	250-1000		300-1000	1000-5000	
3. Arid and polar zones.	1500-10,000			5000-20,000		
4. Homogeneous plains areas.			5000			
5. Less homogeneous regions			2000-3000			
- Arid regions						30,000
- Humid temperate						50,000
- Cold regions						100,000

Table 3.4

Precipitation network data for selected regions - 1971.
(Ferguson, 1973)

REGION	$10^4 km^2$ TOTAL AREA	DAILY PRECIPITATION STATIONS	DENSITY STATIONS/ $10^4 km^2$	SPECIFIC AREA km^2/STATION
Switzerland	4.1	463	112	89
Sweden	44.6	918	20.6	486
Norway	32.4	730	22.5	445
British Columbia, Canada	94.1	380	4.1	2480
Utah, U.S.A.	21.2	166	7.8	1280

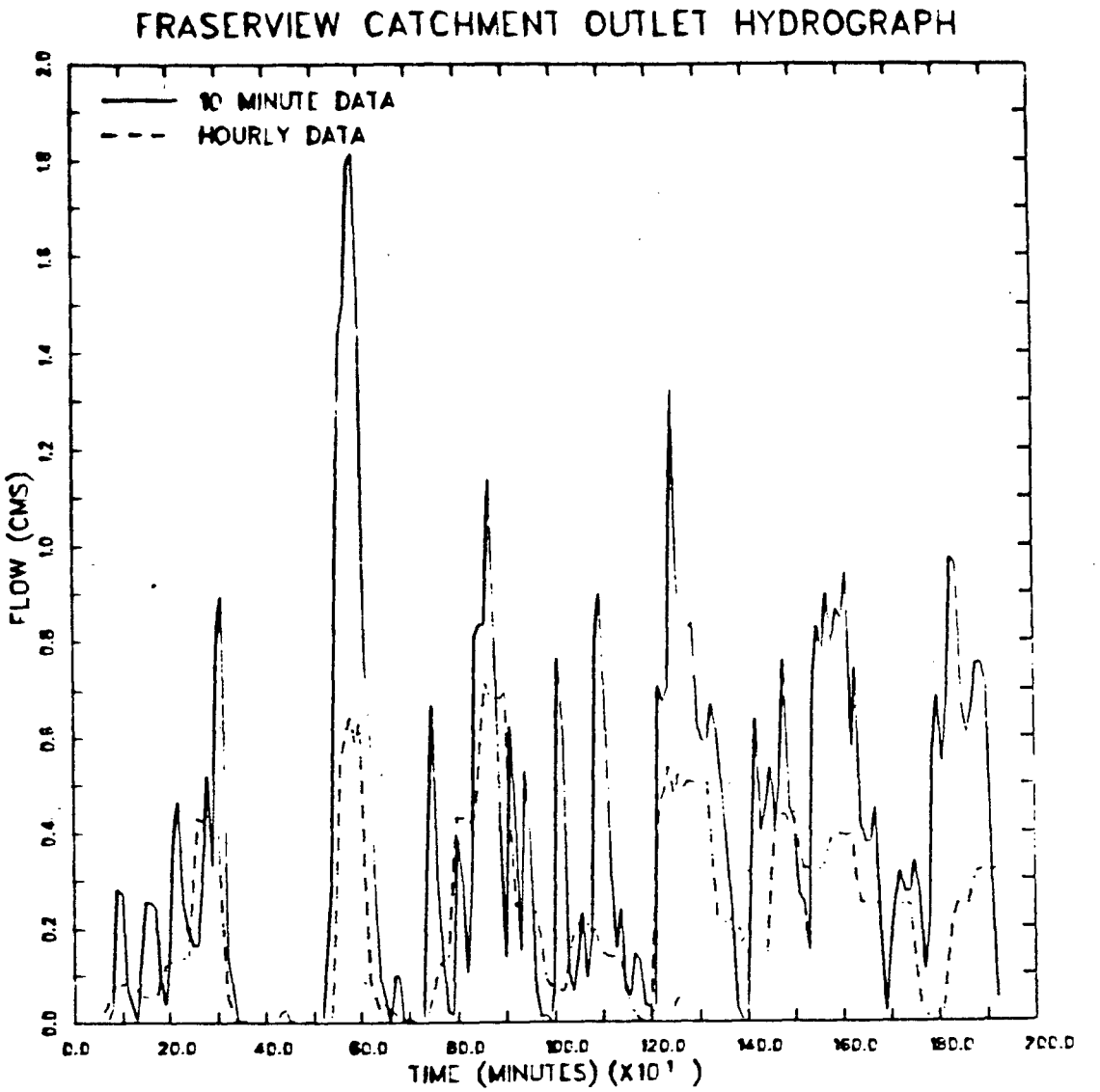

Figure 3.1. Comparison of SWMM hydrographs from ten minute radar and equivalent hourly gauge data (Bonser, 1982).

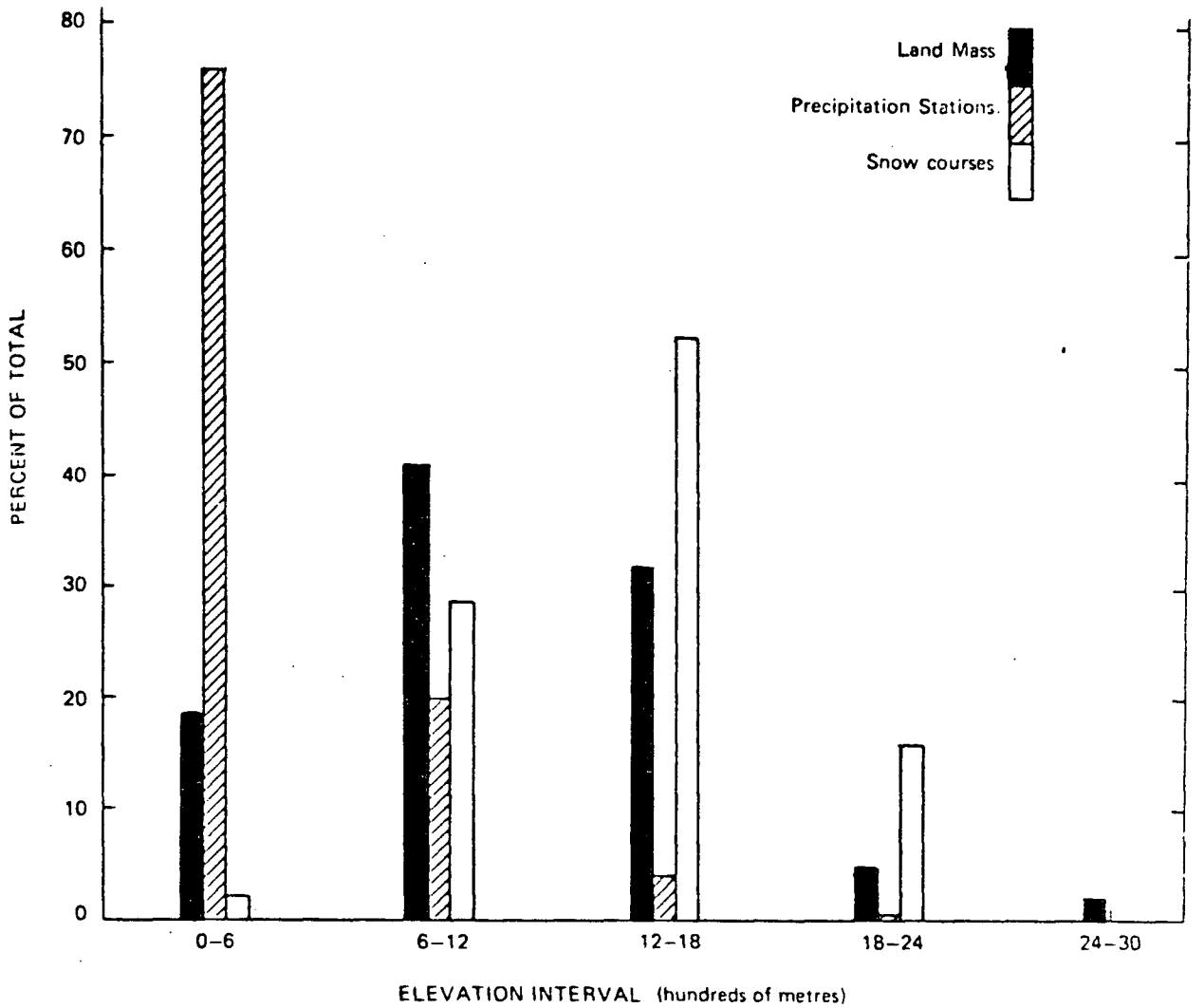

Figure 3.2. Relative distributions of land area, precipitation stations and snow courses by elevation interval in British Columbia. In early 1971 there were 370 precipitation stations and 215 snow courses in operation (Ferguson, 1973).

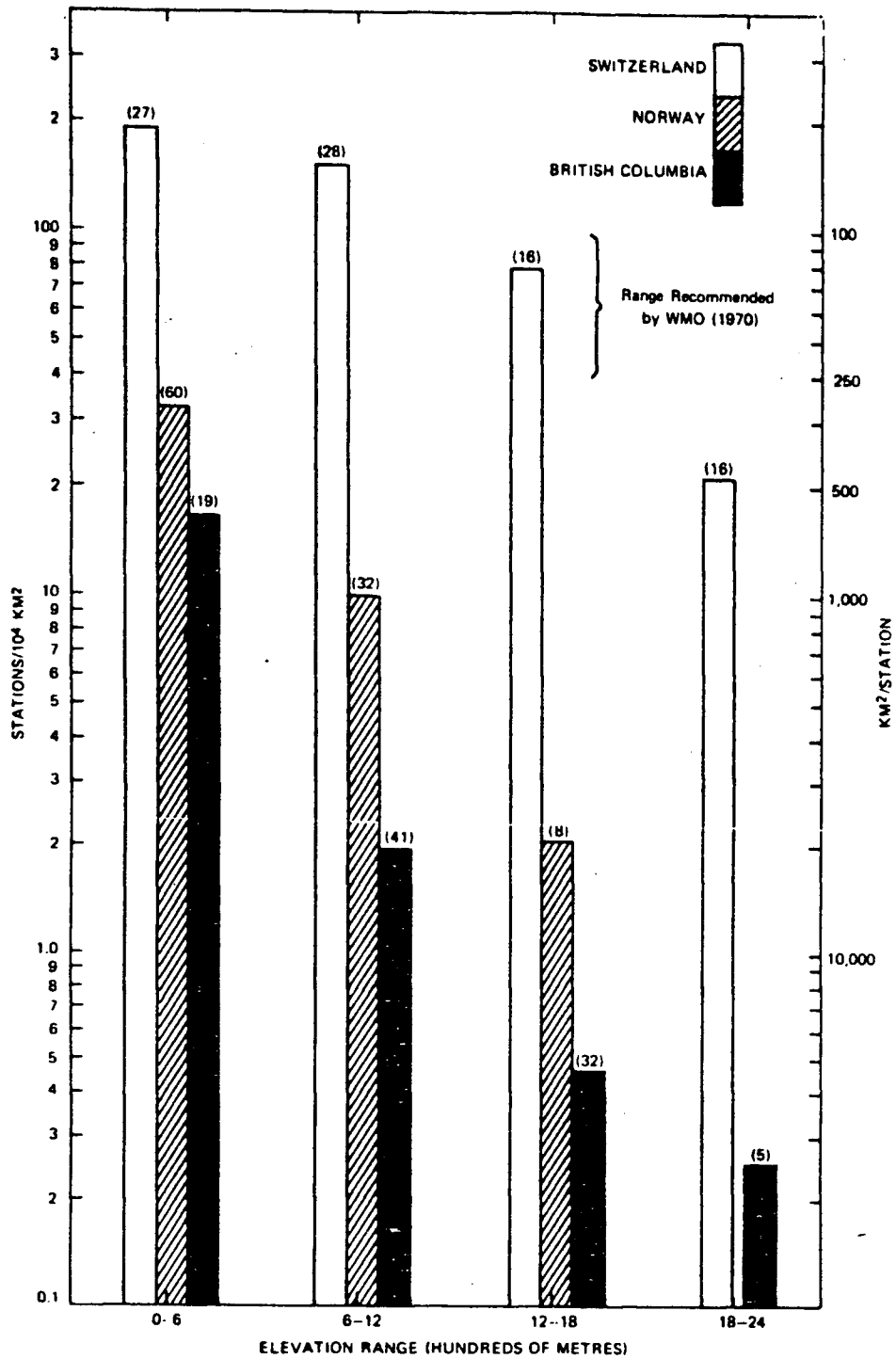

Figure 3.3. Densities of precipitation networks (daily reporting stations, 1971) by elevation interval in Switzerland, Norway and British Columbia. Figures in brackets represent percentages of the total area of each region falling in the elevation range. For example 41 per cent of British Columbia is in the range 600 to 1200 metres (Ferguson, 1973).

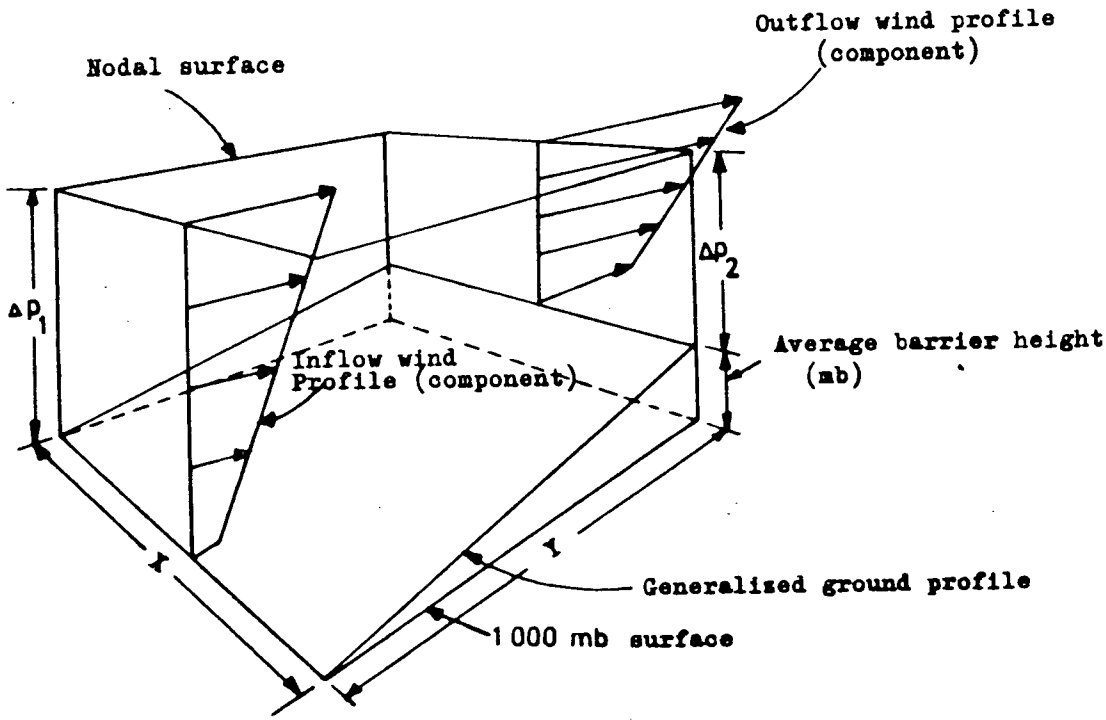

Figure 3.4. Simplified inflow and outflow wind profiles over a mountain barrier.

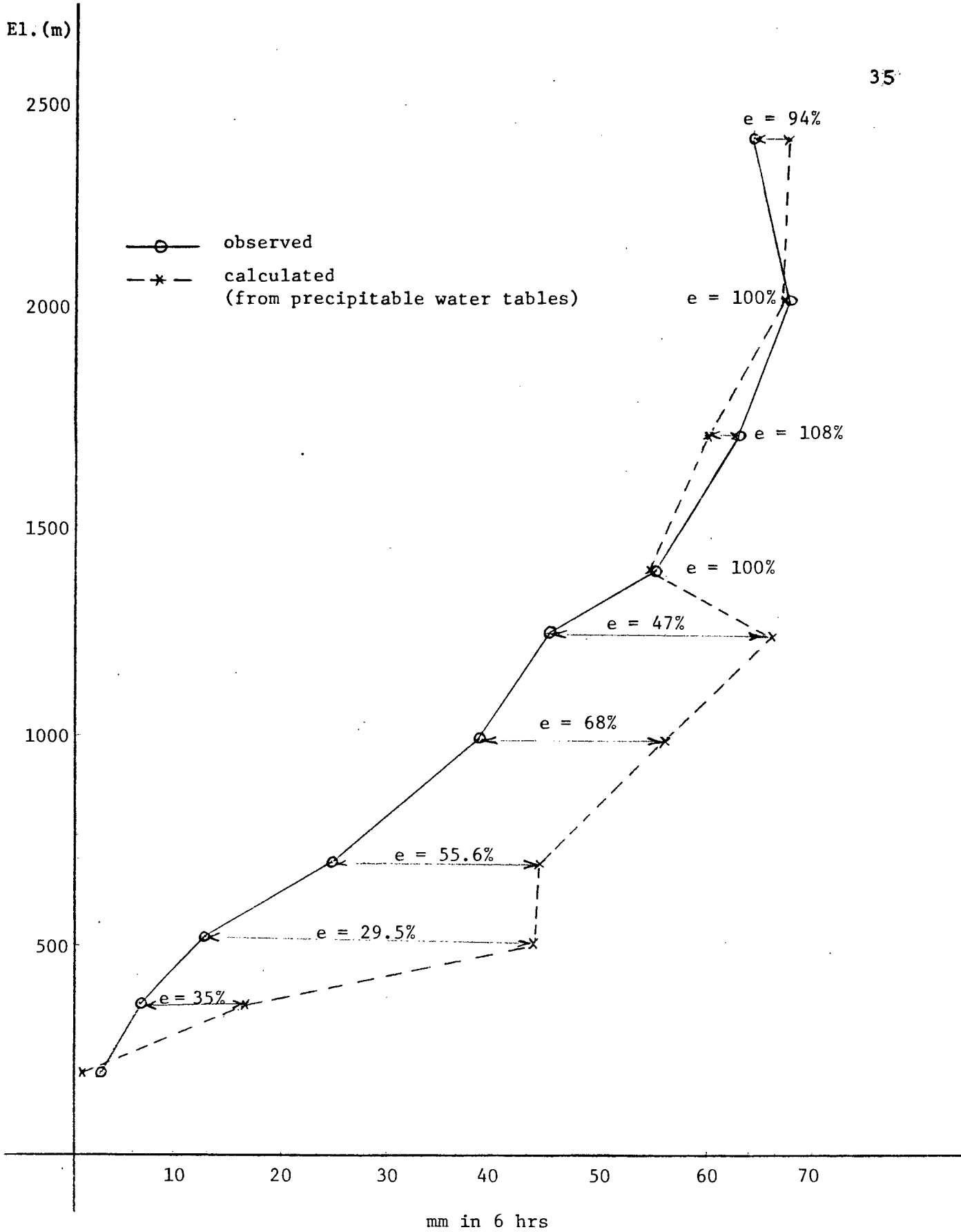

Figure 3.5. Data from W.M.O. (1973), p. 64.

CHAPTER 4

DEBRIS TORRENT MOVEMENT

4.1 Massive Sediment Motion

A debris torrent is a form of massive sediment motion which means the falling, sliding or flowing of conglomerate or the dispersion of sediment, in which all particles as well as the interstitial fluid are moved by gravity, so that the relative velocity between the solid phase and fluid in the direction of displacement of mass plays only a minor role. By contrast, in fluid flow, lift and drag forces due to relative velocity are essential for individual particle transport.

4.2 Initiation of Movement in Torrent Stream

Once sufficient material from the debris source area is deposited in the stream bed, the channel is then a potential debris torrent given the right conditions of slope and precipitation.

Imagine a thick uniform layer of loosely packed non-cohesive grains, whose slope angle is θ. It is assumed that at the moment when surface flow of water of depth h_0 appears the pore spaces are saturated and parallel seepage flow occurs. The characteristic distribution of shear stress in the bed is like that shown in Fig. 4.1, in which τ is the applied tangential stress and τ_L the internal resistive stress.

Case 1 (Fig. 4.1a) occurs under the condition (Takahashi, 1981),

$$\tan\theta \geq \frac{C_*(\sigma-\rho)\tan\phi}{C_*(\sigma-\rho)+\rho} \qquad (4.1)$$

in which

C_* = grain concentration by volume in the static debris bed.

σ,ρ = densities of grains and fluids respectively

ϕ = internal friction angle

When case 2 occurs (Fig. 4.1b) the following equation should be satisfied

$$\tan\theta = \frac{C_*(\sigma-\rho)}{C_*(\sigma-\rho) + \rho(1+h_0 a_L^{-1})} \tan\phi \qquad (4.2)$$

in which a_L is the depth where τ and τ_L coincide.

The whole bed in case 1 and the part above the depth a_L in case 2 will begin to flow as soon as the surface flow appears. This type of instability in the bed is due not to the dynamic force of fluid flow but to static disequilibrium, so that the flow should be called sediment gravity flow.

The condition for occurrence of sediment gravity flow is therefore, $a_L \geq d$ in which d is the grain diameter. Substitute this condition into Equation (4.2) and we obtain

$$\tan\theta \geq \frac{C_*(\sigma-\rho)}{C_*(\sigma-\rho) + \rho(1+h_0 d^{-1})} \tan\phi \qquad (4.3)$$

but when a_L is far less than h_0 grains cannot be uniformly dispersed throughout the whole depth due to rather small colliding dispersibility. Therefore a sediment gravity flow that is appropriately called debris torrent should meet the condition $a_L \geq Kh_0$, in which K is a numerical coefficient, determined from experiment to be about 0.7. Substituting the condition $a_L \geq Kh_0$ into Equation (4.3) gives

$$\tan\theta \geq \frac{C_*(\sigma-\rho)}{C_*(\sigma-\rho) + \rho(1+k^{-1})} \tan\phi \qquad (4.4)$$

Debris movement occur when Equations (4.3) and (4.4) are simultaneously satisfied.

4.3 Suspension of Massive Material

The debris torrent phenomenon occurs in surges spaced over several hours (Hungr et al., 1984). A typical surge through the lower reaches of a mountain creek begins by the rapid passage of a steep bouldery front, followed by the main body of the torrent. This consists of coarse particles ranging from gravel to boulders and logs, apparently floating in a slurry of liquefied sand and finer material. The inclusion of debris larger than could be expected to be moved by normal hydraulic forces and the mechanism of such transport requires upward sediment-supporting forces that turbulence of the interstitial fluid would be too weak to provide.

Bagnold (1954) proved the existance of a dispersive pressure resulting from the exchange of momentum between the grains in neighbouring layers. When the voids are filled by dense clay slurry, large stones can be dispersed under rather small dispersive pressure, helped by bouyancy in the fluid phase.

Bagnold also investigated the effect of dispersion of large solid spheres on the shear resistance of a Newtonian fluid. He held that in a situation where a stream is transporting granular material, the only explanation was a dispersive grain pressure of such a magnitude that an

appreciable part of the moving grains is in equilibrium between it and the force of gravity.

4.4 Bagnold's Dilatant Fluid Model

A dispersion of neutrally bouyant particles were sheared in a Newtonian fluid in the annular space between two concentric drums. The particles dilated to the extent of exerting pressure on the vertical walls perpendicular to the main flow. Bagnold reasoned that this dispersive pressure is the result of momentum exchange associated with grain encounters and he found that the dispersive pressure is proportional to the shear stress. When the applied shear strain du/dy is small the resulting shear stress is a mixed one due to the effect of fluid viscosity as modified by the presence of grains, whereas when the applied shear strain is large the viscosity of the interstitial fluid is insignificant and the resulting shear stress is essentially due to grain interaction. For the latter case Bagnold found

$$P = a\,\sigma[(C_*/C_d)^{1/3}-1]^{-2}\,D^2(du/dy)^2\cos\alpha$$

$$T = P\tan\alpha \qquad (4.5)$$

P = dispersive pressure

T = shear stress

α = dynamic angle of internal friction

a = numerical constant = 0.042

D = grain diameter

It should be noted that the density ρ of the interstitial fluid does not enter into Equation (4.5). If a single solid body is moved through a fluid, the total rate of momentum transfer is measured by $(\sigma-\rho)$ because the fluid tends to flow back around the body to take its place. In this case however, it seems unlikely that "its place" can have a physical meaning, since the whole surrounding configuration changes during the grains' movement. It was assumed therefore that the movement of the displaced fluid is of a random nature in relation to the movement of the grains.

Bagnold's experiment shows that the fully inertial condition is satisfied at:

$$G^2 = \sigma D^2 T \left[(C_*/C_d)^{1/3}-1\right]\mu^{-2} > 3000 \qquad (4.6)$$

where μ is fluid viscosity and G has the form of a Reynolds number or in terms of the conventional Reynolds number

$$R > 55$$

This condition should easily be met in a debris torrent situation.

Bagnold reasons that when grains of mixed sizes are sheared together the larger grains tend to drift towards the free surface, because for a given shear strain the dispersive stress appears to increase as the square of the size (Eq. 4.5). Since the flow surface moves fastest, the larger material should drift towards the front of the flow, thus explaining the bouldery front that is characteristic of the debris torrent.

4.5 Plastico-Viscous Rheological Models

Another set of studies (Johnson, 1970; Middleton and Hampton, 1976; Rodine and Johnson, 1976) propose the use of a Bingham plastic fluid model since the flow of clay slurry is well modelled as a Bingham fluid.

The stress-strain relationship in a Bingham fluid is

$$\tau = \tau_y + \mu \, du/dy$$

where

τ = shear stress

τ_y = yield strength

μ = viscosity

Middleton and Hampton (1976) distinguished debris flow from grain flow. They emphasize that the dispersive stress due to direct grain interaction plays an important role only in the case of grain flow, and that in the case of debris flow; the grains are supported by matrix strength, and the viscosity of the interstitial fluid determines their hydraulic behaviour. They further claim that only a slight amount of clay in the interstitial fluid will drastically influence grain flow and convert it into debris flow.

It should be noted that the above refers to debris flow and the phenomenon under consideration should be distinguished from a debris torrent proper. It is possible for a Bingham fluid to flow in a channel of very low slope if the depth of flow is large enough, this is not in accordance with a real debris torrent.

To avoid the contradiction of this low slope flow, Johnson (1970) proposed a Coulomb-viscous model in which the stress-strain relationship is:

$$\tau = C + \sigma_n \tan\phi + \mu \, du/dy$$

C = cohesion

σ_n = normal stress

ϕ = angle of internal friction

This model, as did the Bingham fluid, still attributes the transport of large boulders to their bouyancy due to the strength of the interstitial clay slurry. Hampton (1975) obtained experimental relationships bewteen the clay contents in clay-water slurry and the competence to float grains. These results show that sand sized particles can be floated but larger ones cannot.

4.6 Evaluation of Models

Takahashi (1980) re-evaluates the role of clay content in the ordinary grain-rich debris and emphasizes that the effects of clay are minor and consequently the flow is dilatant. He concludes:

- Ordinary grain-rich debris contains much less clay component for it to be treated as a Bingham fluid. The apparent high viscosity should be the result of the resistance caused by collisions of particles.
- Debris flows of the ordinary scales may be modelled by Bagnold's grain flows in the fully inertial range.

The debris torrent is of course a debris flow in the fully inertial range. However it is important to draw the distinction between the clay

charged mudflow that is modelled as a Bingham fluid and the debris torrent phenomenon that appears best modelled as a dilatant fluid.

As shown in Fig. 4.2, the domain of occurrence of various types of sediment transportation are defined by Equations 4.1, 4.2, 4.3, and 4.4, the condition for fall ($\theta=\phi$), and the equation of critical tractive force on a steep channel (Ashida et al., 1973)

$$\frac{\rho u_{*c}^2}{(\sigma-\rho)gd} = 0.034 \cos\theta \left[\tan\phi - \frac{\sigma}{(\sigma-\rho)} \tan\theta\right] \times 10^{0.32(d/h_0)}$$

where

u_{*c} = critical shear velocity $[=(gh_0\sin\theta)^{0.5}]$

g = acceleration due to gravity.

The domain labelled 1 is that of no particle movement; 2 is the domain of individual particle movement due to the dynamic force of fluid flow, i.e. bed transport; 3 is the domain of sediment gravity flow, in which the effect of dynamic force of fluid flow coexists and in the flow there is a clear water layer over a dense mixture of grain and water. Numbers attached to the curves in this domain correspond to the thickness of the moving layer of grains. The effect of dynamic action should decrease for increasing thickness of the moving layer. Note that the domains of the transition and the upper regime in the bed form contain both domains of individual particle movement and sediment gravity flow; 4 is the domain of debris flow in which the grains are dispersed in the whole layer (debris torrent); 5 is the domain of the occurrence of both landslides and debris torrents; and 6 the sediment bed is unstable under no fluid flow.

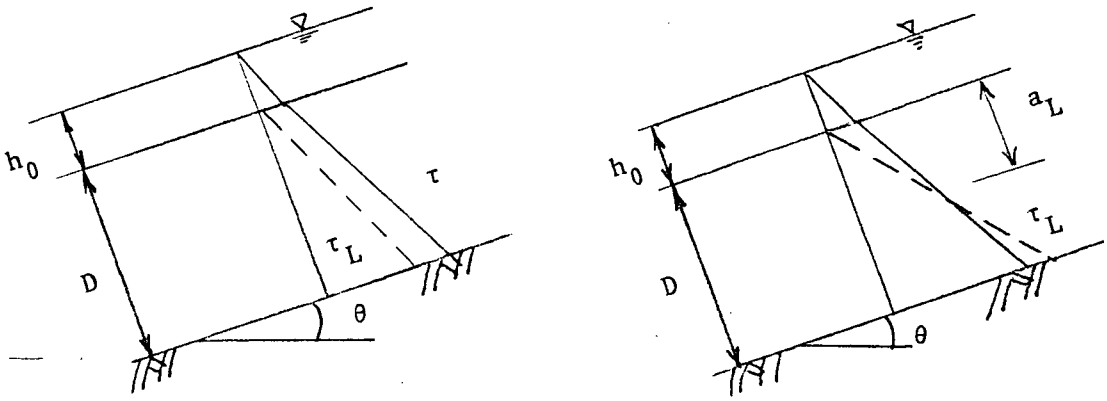

(a) Case 1 (b) Case 2

Figure 4.1 Characteristic shear-stress distribution.

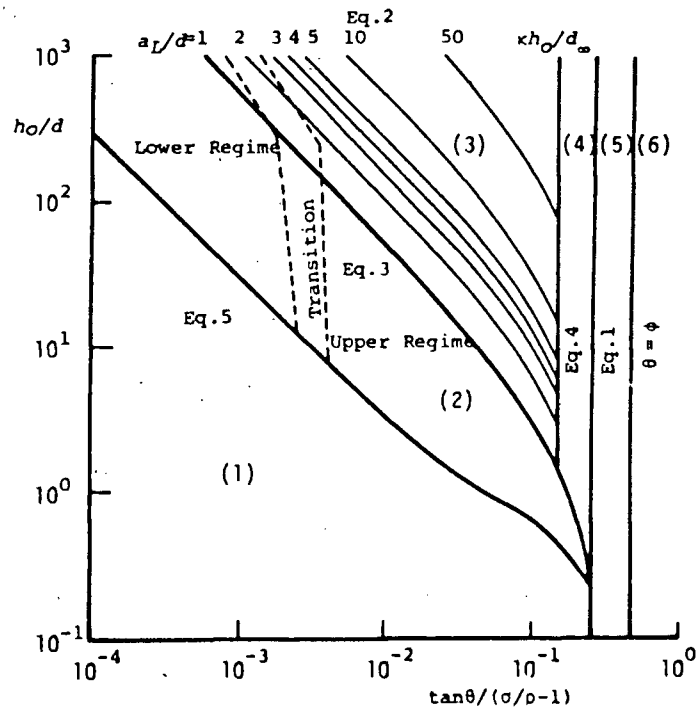

Figure 4.2. Criteria for occurrence of various types of sediment transportation. The curves are obtained under the condition that $c_* = 0.7$, $\sigma = 2.65$ gcm^{-3}, $\rho = 1.0$ gcm^{-3}, $\kappa = 0.7$, and $\tan\phi = 0.8$.

CHAPTER 5

FLOW REGIME OF A DEBRIS TORRENT

Hungr et al. (1984) plotted velocity depth profiles for laminar and turbulent flows in water and compared these with that of debris torrents, using eyewitness reports and superelevation data to establish velocities for the torrent flows (Fig. 5.1). The profiles suggested that the debris torrent flow was much closer to laminar than turbulent flow. However observation of video tapes of debris torrents in motion would suggest that the torrent flow is extremely turbulent. These video tapes were filmed by the C.B.C. at Charles Creek, Howe Sound and by a Japanese research group on a Japanese creek. Consequently the decision was made to examine the phenomenon mathematically, assuming the Bagnold (1954) dilatant fluid theory which implies a totally inertial, i.e. turbulent regime.

5.1 Dilatant Flow

Bagnold (1954) gives the relation for shear stress as

$$\lambda \, D \, \frac{du}{dy} = \left(\frac{\tau}{\delta}\right)^{1/2} \qquad (5.1)$$

where

λ = linear concentration of particles

D = particle size

τ = shear stress

δ = density of mixture.

This equation is similar to the well known boundary layer theory of Prandtl except that the mixing length is assumed to depend on particle size D and not to vary with distance from the boundary Equation 5.1 can be integrated if it is assumed that the shear stress τ is constant, i.e.

$$u = \left(\frac{\tau}{\delta}\right)^{1/2} \frac{1}{\lambda D} \cdot y + C$$

However to be correct τ varies linearly with depth so that

$$\tau = \tau_o - K \cdot y$$

when

$$y = y_{max} \quad \tau = 0$$

$$\therefore \quad y_{max} = \frac{\tau_o}{K}$$

so

$$\tau = \tau_o - \tau_o \frac{y}{y_{max}}$$

$$\tau = \tau_o \left(1 - \frac{y}{y_{max}}\right)$$

Substituting in 5.1 and integrating we obtain

$$u = \frac{\tau_o^{1/2}}{\lambda D \delta^{1/2}} \left(1 - \frac{y}{y_{max}}\right)^{3/2} \cdot 2/3 \left(-y_{max}\right) + C$$

at the boundary $u = 0$, $y = 0$

$$0 = \frac{\tau_o^{1/2}}{\lambda D \delta^{1/2}} (1) \cdot 2/3 \left(-y_{max}\right) + C$$

$$\therefore \quad C = 2/3 \; \frac{\tau_0^{1/2}}{\lambda \, D \, \delta^{1/2}} \cdot y_{max}$$

then

$$u = 2/3 \; \frac{\tau_0^{1/2}}{\lambda \, D \, \delta^{1/2}} \; (1 - \frac{y}{y_{max}})^{3/2} \; (-y_{max}) + 2/3 \; \frac{\tau_0^{1/2}}{\lambda \, D \, \delta^{1/2}} \cdot y_{max}$$

$$\therefore \quad u = 2/3 \; \frac{\tau_0^{1/2}}{\lambda \, D \, \delta^{1/2}} \; y_{max} \; \{[-1 + \frac{y}{y_{max}}]^{3/2} + 1\} \qquad (5.2)$$

let

$$2/3 \; \frac{\tau_0^{1/2}}{\lambda \, D \, \delta^{1/2}} \; y_{max} = A \text{ a const.}$$

or

$$u = A[(-1 + \frac{y}{y_{max}})^{3/2} + 1]$$

$$\frac{u}{A} = 1 - (1 - \frac{y}{y_{max}})^{3/2}$$

when $u = u_{max}$, $y = y_{max}$

so 5.2 yields

$$u_{max} = 2/3 \; \frac{\tau_0^{1/2}}{\lambda \, D \, \delta^{1/2}} \; y_{max} = A$$

$$\therefore \quad \frac{u}{u_{max}} = 1 - (1 - \frac{y}{y_{max}})^{3/2} \qquad (5.3)$$

we may plot this relationship to determine a velocity depth profile for the assumed turbulent conditions of dilatant flow as shown in Fig. 5.2. A similar treatment was used assuming laminar condition of

$$\tau = \mu \frac{du}{dy}$$

which yields the relationship

$$\frac{u}{u_{max}} = +1 - (1 - \frac{y}{y_{max}})^2 \qquad (5.4)$$

which is also plotted in Fig. 5.2

Experimental results given by Daily (1966, p. 235) for turbulent flow were also transposed to the same graph (Fig. 5.2).

The results of this mathematical treatment give a similar profile as that derived by Hungr et al. (1984), from eyewitness reports and superelevation data. We are confronted by a paradox here in that the dilatant flow condition were turbulent but yield what appears to be an almost laminar profile. To accept this as a laminar flow however must be erroneous and the implications of this velocity distribution will now be analyzed.

5.2 Flow Around Bends

Many estimates of the velocity of debris torrents have been made from superelevation data, collected from bends in the torrent channel using the equation,

$$\frac{dh}{dR} = \frac{V^2}{gR} \qquad (5.5)$$

Henderson (1966, p. 255).

where h is the height of the free surface above the horizontal bend,

R = radius of bend

In which equation V is assumed constant with depth which is close to that of actual turbulent flow in water (see Fig. 5.2).

For an open channel V is also assumed to vary as a free vortex, i.e.

$$VR = C \tag{5.6}$$

If R is large enough to assume V constant with radius this gives

$$\Delta h = \Delta R \frac{V^2}{gR} \tag{5.7}$$

where

Δh is total superelevation

ΔR is width of channel

A more exact integration of Eq. 5.3 gives

$$h_2 - h_1 = \frac{C^2}{2g} \left[\frac{1}{R_1^2} - \frac{1}{R_2^2}\right] \tag{5.8}$$

Now the velocity distribution found from the dilatant flow is almost linear with depth, so we may assume that the actual relationship of velocity with depth is

$$V = ky$$

i.e.,

$$\frac{dh}{dR} = \frac{k^2y^2}{gR}$$

Integration over the depth gives

$$\int_o^Y (\frac{dh}{dR})dy = \int_o^Y \frac{k^2y^2}{gR}\, dy$$

at fixed radius assuming dh/dR to be constant with depth

$$y\,\frac{dh}{dR} = \frac{k^2}{gR} \cdot \frac{1}{3}\, Y^3$$

$$\frac{dh}{dR} = \frac{k^2}{gR} \cdot \frac{1}{3}\, Y^2 = \frac{1}{3}\,\frac{k^2h^2}{gR}$$

for horizontal channel, for which Y=h.

Integrating from R_1 to R_2 and h_1 to h_2 gives

$$\frac{1}{h_1} - \frac{1}{h_2} = \frac{k^2}{3g}\, \ell n\, \frac{R_2}{R_1} \qquad (5.9)$$

To illustrate the numerical results of these equations we take some assumed values, i.e.,

$$h_{av} = 1 \text{ m}, \quad V_{av} = 5 \text{ m/sec}, \quad \Delta R = B = 5 \text{ m}$$

with

$$R_M = 42.5$$

and substitute in Eq. 5.8 we get

$$\Delta h = 0.3 \text{ m}$$

from Eq. 5.9 we have

$$\frac{\Delta h}{h_1 h_2} = \frac{k^2}{3g} \ln \frac{R_1}{R_2}$$

The maximum velocity, $V_M = k \cdot y_m$. Therefore $k^2 h_1 h_2 = V_M^2$, so that,

$$\Delta h \simeq \frac{V^2}{3g} \ln \frac{R_1}{R_2}, \quad \text{i.e. } k^2 \, h_1 h_1 \simeq V^2$$

gives

$$V_M = 8.65 \text{ m/sec}$$

Which shows that the near linear velocity distribution for dilatant flow yields a much higher velocity from superelevation data than the usually assumed Eqn. 5.7.

Hungr et al. (1984) quote the equation

$$\Delta h = K \cdot \frac{B \, V^2}{Rg}$$

where B is surface with of flow, and K is given by Myzuyama et al. (1981) to range from 2.5 to 5.0 and the 2.5 value is used to estimate velocities from the equation,

$$\Delta h = \frac{2.5}{Rg} \cdot B \, V^2$$

for the same Δh, this equation yields

$$V = 3.16 \text{ m/s}$$

which is much lower than the value 8.65 m/sec estimated above. No justification of the 2.5 factor is given. Also, Professor M. Sugawara (National Research Centre for Disaster Protection, Kyoto, Japan) recently read Myzugama's paper in the original Japanese and reported that there was no justification of the 2.5 factor in the paper.

For design purposes these estimated velocities are used to calculate impact forces using the momentum equation (Hungr et al., 1984),

$$F_T = \delta A V^2 \sin\beta, \quad \text{i.e.} \quad F_T = \delta Q V \sin\beta$$

where

F_T = total thrust

A = flow cross-section

δ = debris density

β = angle of flow direction to face of barrier.

This velocity difference would increase the thrust force by a multiple of 7.5. It should be noted from Ippen and Knapp (1938) that at highly supercritical flows Δh could be as much as twice that estimated by Eq. (5.4). However the Froude number range we are investigating is generally low enough to have a minimal effect on our calculated velocity, for example, at a Froude number of 1.6, (a high value for debris torrent flow) Δh would increase by 35% reducing the estimated velocity by 14%.

5.3 Further Applications of Turbulent Flow

Again if we accept Bagnolds inertial range for debris torrent and agree that turbulent conditions prevail then we can apply Reynold's

(1884) turbulent stress analysis to the flow, this may have applications to the runout zone of the torrent, which can have important design applications, particularly with respect to zoning.

5.4 Turbulent Stress

At any given point in turbulent flow, the instantaneous velocity and indeed all the instantaneous continuum properties are found to fluctuate rapidly and randomly about a mean value with respect to time and spatial direction. In the theoretical analysis of turbulent flow, it is convenient to consider an instantaneous quality such as u, as the sum of its time averaged part $\bar{u}$ and momentary fluctuation part u' as shown in Fig. 5.3, i.e.,

$$u = \bar{u} + u'$$

In steady flow $\bar{u}$ does not change with time.

By definition

$$\bar{u} = \frac{1}{t_0} \int_0^{t_0} u \, dt$$

$$\bar{u}' = \frac{1}{t} \int_0^{t_0} u' \, dt = 0$$

Although the time average of fluctuation quantity is zero, i.e. $\bar{u}' = 0$, the quantity $\overline{u'^2}$, $\overline{u'v'}$, $\overline{u'w'}$, etc. which are time averages of the products of any two fluctuation components, will not necessarily equal zero. These values are used as a measure of the magnitude of turbulent fluctuations at any given point in a turbulent flow field, i.e. the intensity of turbulent I is defined by

$$I = \frac{\sqrt{\bar{u}'^2 + \bar{v}'^2 + \bar{w}'^2 \,/3}}{u}$$

where u is the magnitude of the velocity at the same point.

We may consider the turbulent component at right angles to the flow u as $\sqrt{\bar{v}'^2}$ which we will call v' the root mean square turbulent velocity in the lateral direction. This v' value will be used to estimate lateral spreading when the torrent leaves the constraints of the channel. We can calculate this component from the turbulent shear stress equation

$$\tau_0 = \gamma_w R_h S_0 = \rho v_*^2 \quad (v_* = \text{shear velocity} = v')$$

where

R_h = hydraulic radius

S_0 = slope

or

$$v' = (g R_{h_0} S_0)^{1/2}$$

From the random nature of this turbulence we may assume a normal distribution so that for any stream parameters a statistical analysis can be done to estimate the potential zone of deposition. This of course, is an ideal situation based on an equal size material but represents the extreme case of maximum spreading. Since when a range of material sizes are deposited we would expect the larger boulders to deposit first and inhibit movement of smaller material. There are some

striking examples of streams carrying ranges of sizes of material, where the larger sized material builds a steep bank or levee on each side, containing the smaller material within these boundaries.

The extreme case can be examined using a normal statistical distribution, to represent the randomness of these turbulent fluctuations. We can predict the range of deposition by recognizing that the lateral velocity fluctuation v' is equivalent to the standard deviation s, so that approximately 68% of the material will move laterally at less than v', while another 27% will move at less than 2v' (see Fig. 5.4).

e.g. In an ideal situation with a channel slope of 20° and an hydraulic radius of 1 and a mainstream velocity of 5 m/s

$S_0 = 36$

$R_{h_0} = 1$

$u = 5$ m/s

then $v' = (9.8.1 \cdot 36)^{1/2}$

$= 1.9$ m/s

giving an angle of spread of $\tan^{-1}(1.9/5) = 21°$

Therefore we would expect 68% of the material to spread at within an angle of 21°.

A further 27% should spread within $\tan^{-1}(3.8/5) = 37°$.

We therefore see that the angle of spreading of a debris torrent when it reaches the fan region is physically limited by the turbulent velocity fluctuations, and only a small portion of debris will spread beyond 20° of the centreline of the torrent.

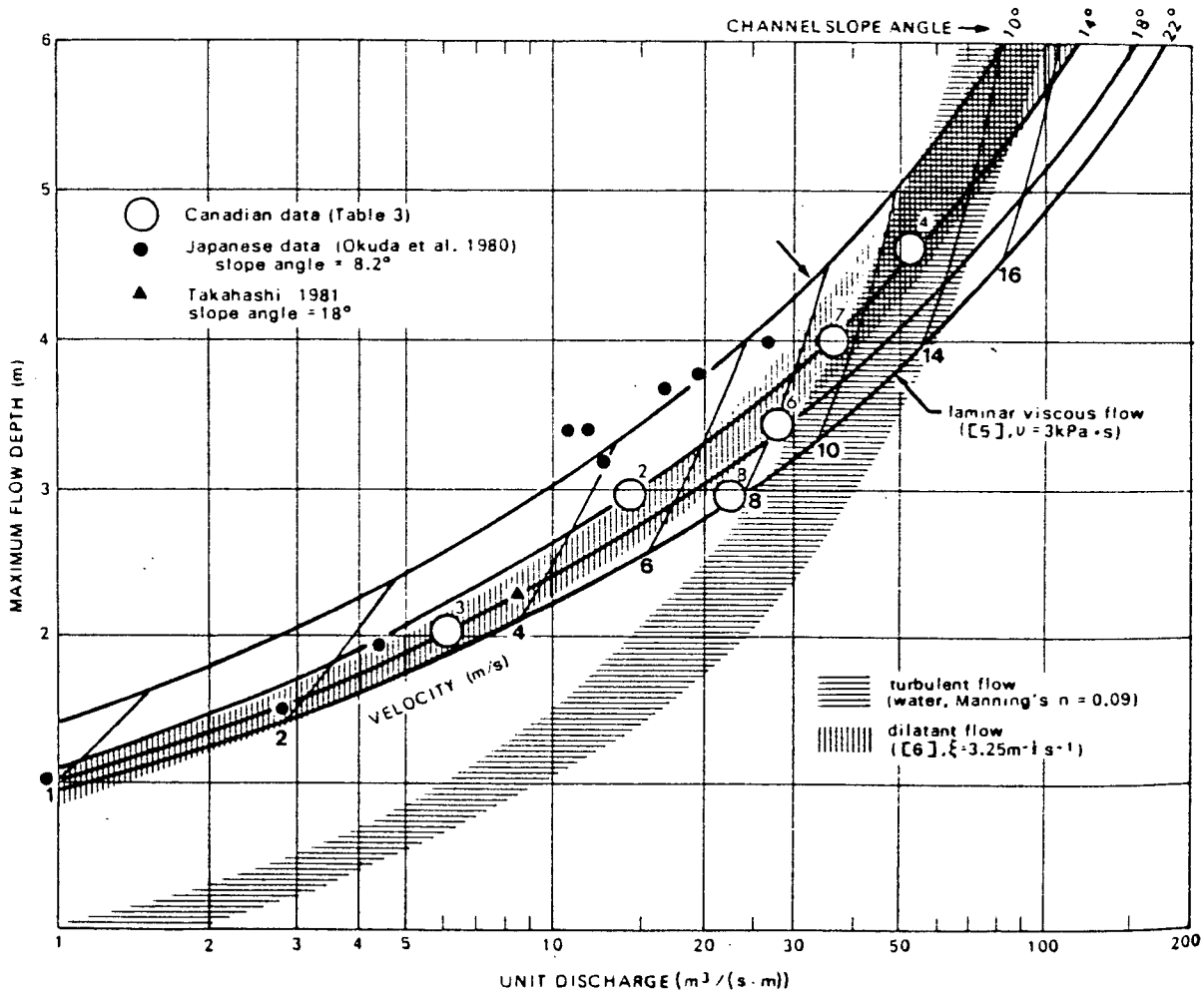

Figure 5.1 Velocity/depth relationships applicable to the peak of debris torrent surge (Hungr et al., 1984).

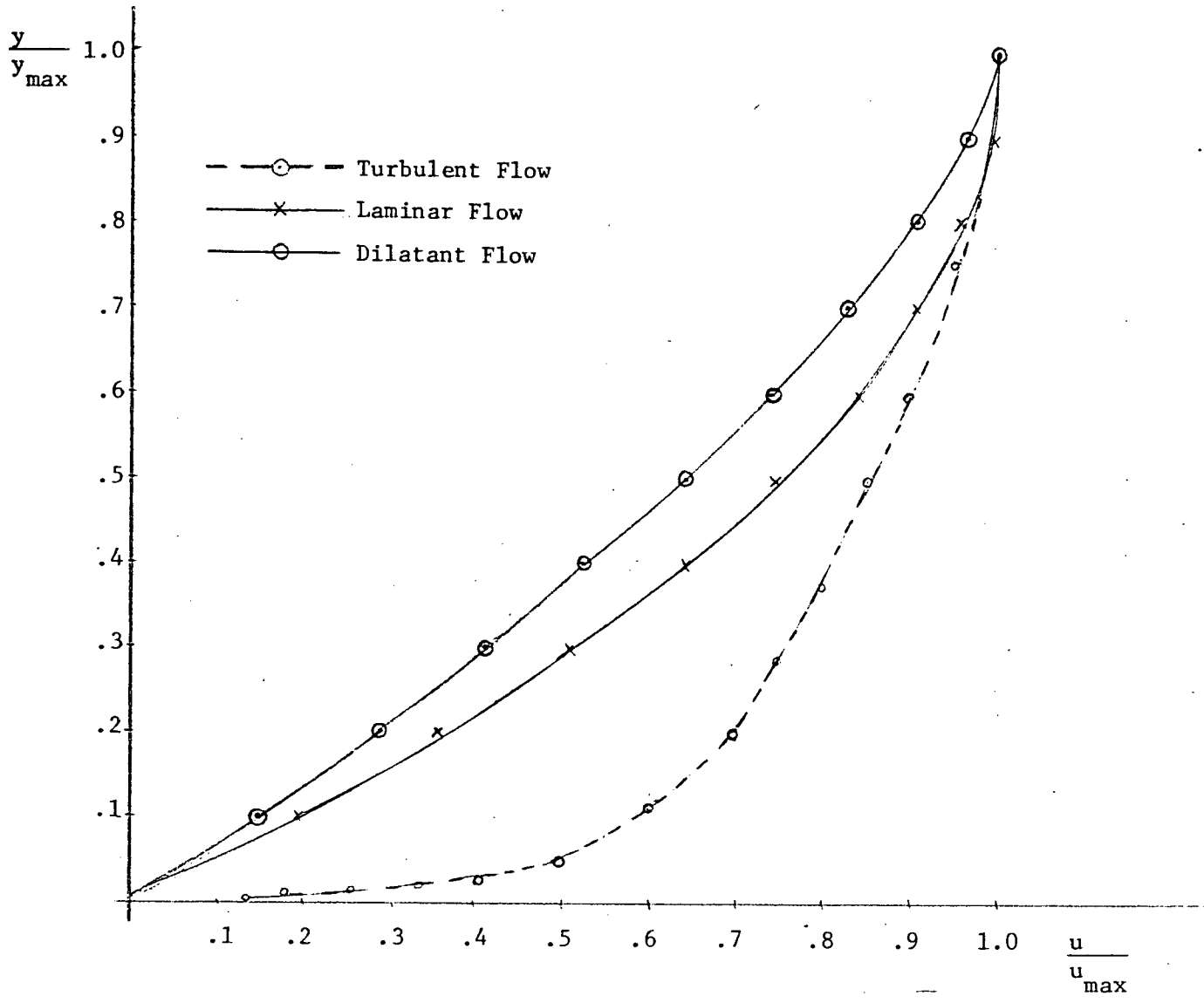

Figure 5.2 Velocity/depth profiles, comparing dilatant flow with laminar and turbulent (theoretical).

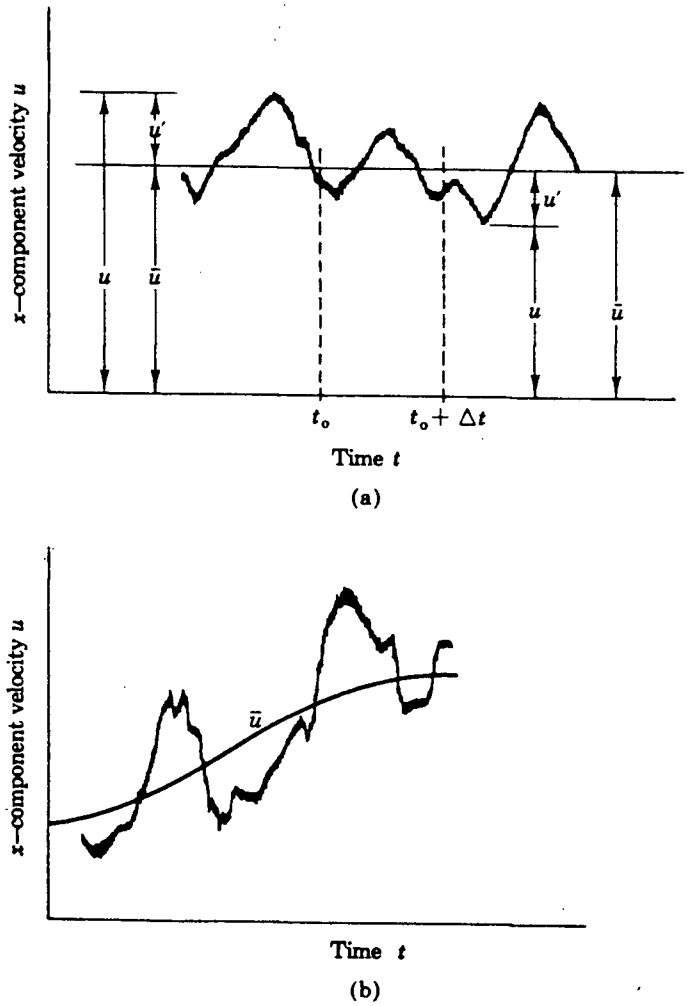

Figure 5.3 Fluctuations of instantaneous velocity component with respect to time at a fixed point in steady flow.

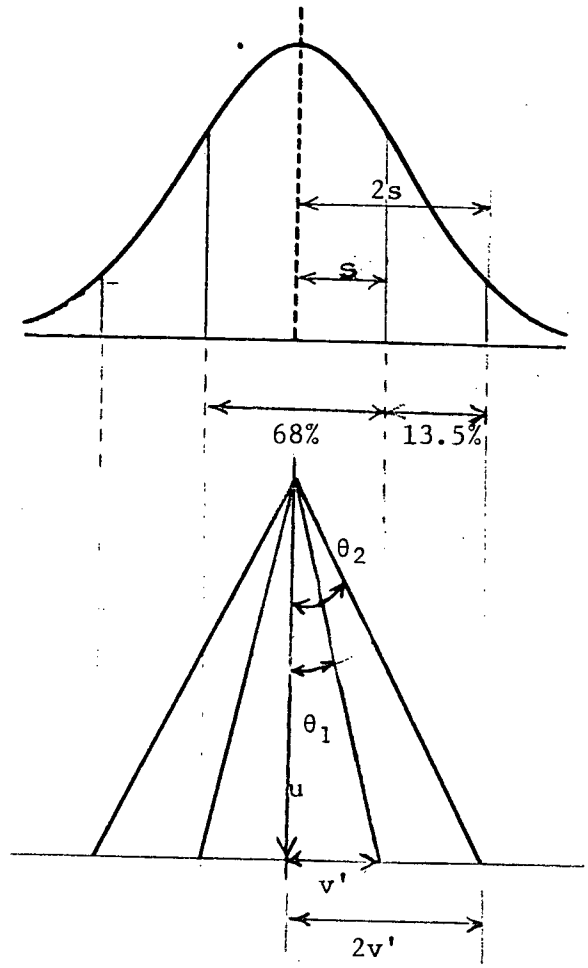

Figure 5.4 Normally distributed lateral velocities giving angles of spread for torrent material.

CHAPTER 6

CONCLUSIONS

A debris torrent is a massive sediment motion in which all particles as well as the interstitial fluid are moved by gravity, this only occurs in steep channels where there is a rapid movement of water charged soil, rock and organic material.

Debris torrent events are usually triggered by debris slides or avalanches from adjacent hill slopes, in the debris source area, which enter a channel and move directly down stream.

Rainfall is the most important factor in the initiation of these debris movements that culminate in debris torrent activity. The type of events that are most critical are, sustained regional rainstorms i.e. 300 mm or more of precipitation in 48 hours or convective cell activity which is responsible for intense bursts of rainfall over short time intervals and may contribute as much as 50 mm of precipitation to the catchment area in one hour.

The effect of the addition of water to the soil mantle and the associated conditions for instability were investigated by Terzaghi (1950) and Skempton and Delong (1957), from the work of the latter a family of curves for various combinations of soil parameters were derived (Fig. 25), from which a critical slope angle β can be estimated. It was noted that this was for an ideal situation and that apparent cohesion due to true cohesion plus root strength of vegetation can alter the factor of safety quite dramatically.

Removal of forest cover in the debris source area by logging was also found to be a major contributing factor, since this decreases root

strength, interrupts surface drainage and changes the distribution of mass on the slope surface by cut and fill construction. In addition shading of snow pack is reduced, increasing the incidence of snow avalanching which can initiate debris movement. It was also concluded that not only the incidence of land movement is increased but rates of erosion can increase markedly due to denudation.

An examination of the precipitation events associated with debris torrents was carried out with particular reference to the precipitation measurement networks and current practice of assuming stationary growth and decay of storms. Due to the sparse data network, in the area of Howe Sound, where most data stations are located along the major transportation routes, much of the actual precipitation in the higher catchments is not reflected in the gauging network. The main components of the precipitation not being picked up by the gauges are those of convective cell activity and the orographic effects of the mountains. In order to use data in a predictive fashion to account for this orographic effect a much more comprehensive data collection system is required along with a model to interpret the orographic component. The convective cells can be as small as 1.5 km and would require sophisticated radar tracking for accurate location, as discussed by Bonser (1982).

The data network density in B.C. was compared to other areas of the world and to W.M.O. specifications and was found to fall far below these recommendations.

The mechanism of movement of a torrent was considered, with special reference to the transportation of boulders by the flow. The apparent ease with which these large rocks are moved has been a subject for much

research to date. Two theories were examined, Bagnold's (1954) Dilatant Fluid Model, and Johnson's (1970) Plastico-Viscous Model. Bagnold's model showed that when particles were sheared together the larger particles tended to drift toward the free surface and since the flow surface moves fastest, the larger material drifts toward the front of the flow and is supported by exchanges in momentum with the smaller particles beneath. This model gave a good explanation of the phenomenon observed, where boulders appeared to "float" toward the front of the torrent. The Plastico-Viscous Model proposed that the particles are supported by matrix strength and that the viscosity of the interstitial fluid determines the hydraulic behaviour.

An evaluation of the models revealed that the grain rich debris does not contain enough clay to be treated as a Bingham Fluid (Plastico-Viscous) and that apparent high viscosity was the result of the resistance caused by the collisions of particles. It was concluded that the debris torrent could best be modelled as a dilatant fluid in its fully inertial (turbulent) range.

Other workers, Hungr et al. (1984) have concluded that the debris torrent flow was laminar, due to its apparent calm surface and its velocity depth profile. Hungr et al. plotted velocity vs. depth based on eyewitness reports and superelevation data and found an almost linear relation very close to that of laminar flow. Since the dilatant flow model is a turbulent one it was thought necessary to examine and plot velocity vs depth for this dilatant flow. This dilatant-turbulent velocity profile varies with depth to the power of 1.5, which when plotted is a close approximation to a linear velocity variation. This

contrasts with the logarithmic distribution of normal turbulent flow and the parabolic distribution of laminar flow.

Superelevation of the debris flow in a bend has been used by some workers to estimate flow velocities. Re-analysis of the flow in a bend using the near-linear velocity distribution predicted from the dilatant-turbulent model indicates that the use of conventional superelevation theory may seriously underestimate debris velocities.

Design criteria based on normal fluid flow around bends gave velocities approximately 2.7 times less than these calculation using the linear relation. Further, when these velocities are used to calculate thrust forces which contain a V^2 term the thrust forces would be underestimated by a factor of approximately 7.5. These numerical values are approximate and for illustrative purposes, but they do show the possible range of errors.

This dilatant-turbulent analysis has also been used to estimate lateral spreading of debris torrent material when it spills out laterally from a constrained channel on to the unconstrained debris fan region. An analysis is based on Reynolds turbulent stresses is used to give a statistical estimate of the spread of the debris when it leaves the channel. This statistical analysis can be used to estimate lateral spreading of debris and hence to establish hazard zones on the debris fans.

The most important item revealed in this research is the velocity v depth profile for the dilatant flow, which is very different from what one expects in turbulent flow in water. Further experimental research in this area is needed to continue this analysis and the predicted velocities and thrust forces based on this linear relationship.

REFERENCES

1. Ashida, K., Daido, A., Takahashi, T. and Mizuyama, T. Study on the Resistance Law and the Initiation of Motions of Bed Particles in a Steep Slope Channel: Annual Disaster Prevention Research Institute, Kyoto University 16B 481-94, 1973.

2. Aulitzky, H. Endangered Alpine Regions and Disaster Prevention Measures: Nature and Environment Series 6, Council of Europe, Strasbourg, 103 p, 1974.

3. Bagnold, R.A. Experiments on A Gravity Free Dispersion of Large Solid Spheres in a Newtonian Fluid Under Shear: Proceedings Royal Society of London, Vol. 225A, August 1954.

4. Bonser, J.D. Precipitation Radar as a Source of Hydrometerological Data: M.A.Sc. Thesis, University of British Columbia, 1982.

5. Campbell, R.H. Soil Slips, Debris Flows and Rainstorms in the Santa Monica Mountains and Vicinity, Southern California: U.S. Geological Survey Professional Paper 851, 51 p, 1975.

6. Daily, J.W. and Harleman, D.R.F., Fluid Dynamics: Addison Wesely, 1966.

7. Eaton, C. Flood and Erosion Control Problems and Their Solutions: A.S.C.E. Proceeding, Vol. 62, No. 8, Part 2, Transaction No. 101, 1930.

8. Eisbacher, G.H. Slope Stability and Land Use in Mountain Valleys: Geoscience Canada, Vol. 9, No. 1, 1982.

9. Elliot, R.D. Final Report on Methods for Estimating Areal Precipitation in Mountain Areas: Report 77-13, Department of Commerce, National Oceanic and Atmospheric Administration, National Weather Service Office of Hydrology, 1977.

10. Ferguson, H.L. Precipitation Network Design for Large Mountain Areas: World Meterological Office, 1973.

11. Hampton, M.A. Competence of Fine-Grained Debris Flows: Journal of Sedimentary Petrology 45, No. 4, December 1975.

12. Henderson, F.M. Open Channel Flow: MacMillan Co., Inc., 1966.

13. Hungr, O., Morgan, G.C. and Kellerhals, R. Quantitative Analysis of Debris Torrent Hazards for Design of Remedial Measures: Canadian Geotechnical Journal, 1984.

14. Ippen, A.T. and Knapp, R.T. Experimental Investigation of Flow in Curved Channels: U.S. Engineers Office, L.A. 1938.

15. Johnson, A.M. Physical Processes in Geology: Freeman Cooper, 1970.

16. Kesseli, J.E. Disintegrasting Soil Slips of the Coast Ranges of Central California: Journal of Geology, V. 51, No. 5, p. 343-352, 1943.

17. Lessman, H. and Stamesu, S. Some Rainfall Features in Mountainous Areas of Colombia and their Impact on Network Design: W.M.O. Distribution of Precipitation in Mountainous Areas Symposium, 1973, Vol. 1.

18. Middleton, G.V. and Hampton, M.A. Subaqueous Sediment Transport and Deposition by Sediment Gravity Flow: in Marine Sediment Transport and Environmental Management, Ed. D.J. Stanley, D.J.P. Swift, 11: 197-218, N.Y. Wiley, 1976.

19. Miles, M.J. and Kellerhals, R. Some Engineering Aspects of Debris Torrents: CSCE 5th Canadian Hydrotechnical Conference, 1981.

20. Mizuyama, T. and Uehara, S. Debris Flow in Steep Channel Curves: Japanese Civil Engineering Journal 23, pp. 243-248, 1981.

21. Nasmith, H.W. and Mercer, A.G. Design of Dykes to Protect Against Debris Flows at Port Alice, B.C.: Canadian Geotechnical Journal, Vol. 16, No. 4, pp. 748-775, 1979.

22. Reynolds, O. Experiments Showing Dilatancy: Proceedings Royal Institute of Great Britain (1884-1886).

23. Russell, S.O. Behaviour of Steep Creeks in Large Flood: British Columbia Geographic Series No. 14, Tantalus Research Ltd., 1972.

24. Schaeffer, D.G. A Record Breaking Summer Rainstorm Over the Lower Fraser Valley: Atmospheric Environment Service, Dept. of Environment Canada, Tech. Paper 787, June 1973.

25. Scott, K.M. Origin and Sedimentology of 1969 Debris Flow Near Glendora California: Geological Survey Research Paper No. 750C, p. C242-C247, 1971.

26. Shaw, E.M. A Hydrological Assessment of Precipitation in the Western Highlands of New Guinea: W.M.O. Distribution of Precipitation in Mountainous Areas, Symposium, Vol. II, 1973.

27. Sidle, R.C. and Swanston, D.N. Analysis of Small Debris Slides in Coastal Alaska: Canadian Geotechnical Journal, V. 19, 1982.

28. Skempton, A.W. and Delory, F.A. Stability of Natural Slopes in London Clay: International Conference on Soil Mechanics and Foundation Engineering, 4th London Proceedings, v. 2, p. 378-381, 1957.

29. Swanston, D.N. and Swanson, F.J. Timber Harvesting, Mass Erosion and Steepland Forest Geomorphology in the Pacific North West: Geomorphology and Engineering, Editor Coates, D.R., Dowden, Hutchinson and Ross, Inc., Stroudsburg, Pennsylvania, pp. 199-221, 1976.

30. Takahashi, T. Debris Flow in Prismatic Open Channels: Journal of Hydraulic Division, ASCE, March 1980.

31. Takahashi, T. Debris Flow: Annual Review of Fluid Mechanics, No. 13, pp. 57-77, 1981.

32. Terzaghi, K. Mechanism of Landslides: in Theory to Practice in Soil Mechanics, Wiley & Sons, N.Y., 1960.

33. Thurber Consultants. Debris Torrents and Flooding Hazards on Highway 99, Howe Sound, B.C., April 1983.

34. Whitmore, J.S. The variation of Mean Annual Rainfall with Altitude and Locality in South Africa, as Determined by Multiple Curvilinear Regression Analysis in World Meterological Office: Distribution of Precipitation in Mountainous Areas, Symposium, Vol. 1, 1973.

35. Woods, P.J. Province of British Columbia, Ministry of the Environment, Water Management Branch Memo: March 1, 1983.

36. World Meterological Office. Manual for Estimating of Probable Maximum Precipitation: WMO No. 332, Geneva, Switzerland, 1973.

37. Wright, J.B. Precipitation Patterns Over Vancouver City and Lower Fraser Valley: Meterological Branch, Department of Transport, CIR 4474 TEC 623, 1966.

38. Yoshimo, M.M. Climate in a Small Area: University of Tokyo Press, 1975.